

Extended Higgs Sectors Beyond the Standard Model

WINTER SEMESTER 2018/19

KARLSRUHE INSTITUTE OF TECHNOLOGY (KIT)

LECTURE GIVEN BY

PROF. DR. M. M. MÜHLEITNER

Contents

1	The Standard Model Higgs Sector	1
1.1	The Introduction of the Higgs Boson	1
1.2	The Standard Model Higgs sector	3
1.3	Verification of the Higgs mechanism	5
1.4	Higgs boson decays	5
1.5	Higgs boson production at the LHC	9
1.6	Higgs Boson Discovery	13
1.7	Higgs boson couplings at the LHC	14
1.8	Higgs Boson Quantum Numbers	16
1.9	Determination of the Higgs self-interactions	20
1.9.1	Determination of the Higgs self-couplings at the LHC	20
1.10	Summary	22
2	The 2-Higgs Doublet Model	25
2.1	The Higgs Potential	26
2.2	The problem with flavour conservation	31
2.3	Branching Ratios	34
2.4	Higgs Production	36
2.5	Type II 2HDM and the MSSM	37
2.6	The Scalar Sector of the 2HDM	37
2.6.1	Notations of the Scalar Potential	38
2.6.2	Stability of the 2HDM Potential	39
2.6.3	Vacuum Stability	41
2.6.4	Unitarity Constraints	44
2.6.5	Further Constraints	45
3	Appendix	49
3.1	Beispiel: Feldtheorie für ein komplexes Feld	49
	Bibliography	50

Preliminary Content

This lecture will discuss Higgs sectors of various extensions beyond the Standard Model.

1. Revision of the Standard Model (SM) Higgs Sector
2. 2 Higgs Doublet Model
3. The Minimal Supersymmetric Extension of the SM (MSSM)
4. The Next-to-Minimal Supersymmetric Extension of the SM (NMSSM)
5. Composite Higgs Model

Chapter 1

The Standard Model Higgs Sector

Literature:

1. Recent physics results are presented on the webpages of the LHC experiments ATLAS and CMS.
2. A. Djouadi, “The Anatomy of electro-weak symmetry breaking. I: The Higgs boson in the standard model,” *Phys. Rept.* **457** (2008) 1 [hep-ph/0503172].
3. M. Spira, “QCD effects in Higgs physics,” *Fortsch. Phys.* **46** (1998) 203 [hep-ph/9705337] and “Higgs Boson Production and Decay at Hadron Colliders”, *Prog. Part. Nucl. Phys.* **95** (2017) 98.
4. S. Dittmaier *et al.* [LHC Higgs Cross Section Working Group Collaboration], “Handbook of LHC Higgs Cross Sections: 1. Inclusive Observables,” arXiv:1101.0593 [hep-ph].
5. S. Dittmaier, S. Dittmaier, C. Mariotti, G. Passarino, R. Tanaka, S. Alekhin, J. Alwall and E. A. Bagnaschi *et al.*, “Handbook of LHC Higgs Cross Sections: 2. Differential Distributions,” arXiv:1201.3084 [hep-ph].
6. S. Heinemeyer *et al.* [LHC Higgs Cross Section Working Group Collaboration], “Handbook of LHC Higgs Cross Sections: 3. Higgs Properties,” arXiv:1307.1347 [hep-ph].
7. De Florian *et al.*, “Handbook of LHC Higgs Cross Sections: 4. Deciphering the Nature of the Higgs Sector,” arXiv:1610.07922 [hep-ph].
8. H. E. Logan, “TASI 2013 lectures on Higgs physics within and beyond the Standard Model,” arXiv:1406.1786 [hep-ph].
9. Some material on the SM Higgs sector can also be found in my lectures TTP1 and TTP2 and in my lectures on supersymmetry at colliders.

1.1 The Introduction of the Higgs Boson

There are two reasons for the introduction of the Higgs boson [1, 2] in the Standard Model (SM) of particle physics:

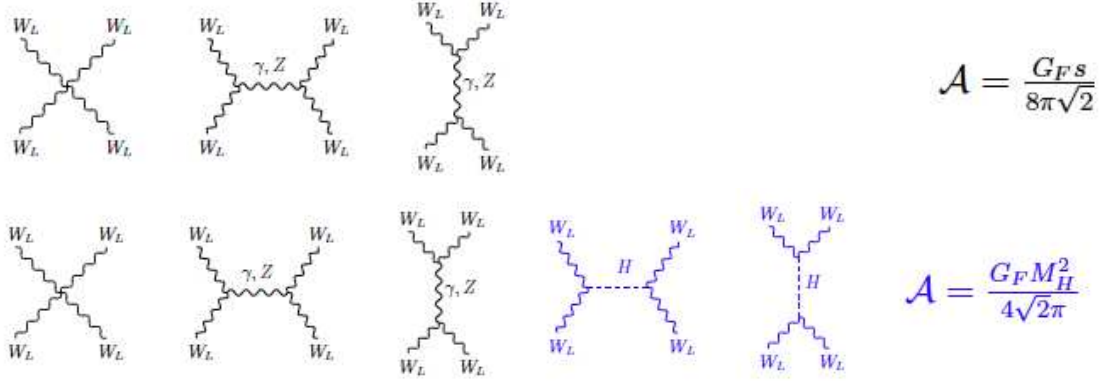


Figure 1.1: The scattering of longitudinal gauge bosons in longitudinal gauge bosons. Upper: without a Higgs boson. Lower: with a Higgs boson

1. A theory of massive gauge bosons and fermions, which is weakly interacting up to very high energies, requires for unitarity reasons the existence of a Higgs particle. The Higgs particle is a scalar 0^+ particle, *i.e.* a spin 0 particle with positive parity, which couples to the other particles with a coupling strength proportional to the mass (squared) of the particles.

Look *e.g.* at the amplitude for the scattering of longitudinal gauge bosons W_L into a pair of longitudinal gauge bosons W_L , see Fig. 1.1. Without a Higgs boson the amplitude diverges proportional to the center-of-mass (c.m) energy squared, s , *cf.* Fig. 1.1 (upper), where G_F denotes the Fermi constant. The introduction of a Higgs boson which couples proportional to the mass squared of the gauge boson, regularizes the amplitude, *cf.* Fig. 1.1 (lower), where M_H denotes the Higgs boson mass.

2. The introduction of mass terms for the gauge bosons violates the $SU(2)_L \times U(1)$ symmetry of the SM Lagrangian. The same problem arises for the introduction of mass terms for the fermions. It violates the chiral symmetry.

Let us have a closer look at point 2. We look at the Lagrangian

$$\mathcal{L}_f = \bar{\Psi}(i\gamma^\mu D_\mu - m)\Psi . \quad (1.1)$$

In the chiral representation the 4×4 γ matrices are given by

$$\gamma^\mu = \left(\left(\begin{array}{cc} \mathbf{0} & \mathbf{1} \\ \mathbf{1} & \mathbf{0} \end{array} \right), \left(\begin{array}{cc} \mathbf{0} & -\vec{\sigma} \\ \vec{\sigma} & \mathbf{0} \end{array} \right) \right) = \left(\begin{array}{cc} 0 & \sigma_-^\mu \\ \sigma_+^\mu & 0 \end{array} \right) \quad (1.2)$$

$$\gamma^5 = \left(\begin{array}{cc} \mathbf{1} & \mathbf{0} \\ \mathbf{0} & -\mathbf{1} \end{array} \right) , \quad (1.3)$$

where σ_i ($i = 1, 2, 3$) are the Pauli matrices. With

$$\Psi = \begin{pmatrix} \chi \\ \varphi \end{pmatrix} \quad \text{and} \quad \bar{\Psi} = \Psi^\dagger \gamma^0 = (\chi^\dagger, \varphi^\dagger) \begin{pmatrix} 0 & \mathbf{1} \\ \mathbf{1} & 0 \end{pmatrix} = (\varphi^\dagger, \chi^\dagger) \quad (1.4)$$

we get

$$\bar{\Psi} i \gamma^\mu D_\mu \Psi = i(\varphi^\dagger, \chi^\dagger) \underbrace{\begin{pmatrix} 0 & \sigma_-^\mu \\ \sigma_+^\mu & 0 \end{pmatrix}}_{\begin{pmatrix} \sigma_-^\mu D_\mu \varphi \\ \sigma_+^\mu D_\mu \chi \end{pmatrix}} \begin{pmatrix} D_\mu \chi \\ D_\mu \varphi \end{pmatrix} = \varphi^\dagger i \sigma_-^\mu D_\mu \varphi + \chi^\dagger i \sigma_+^\mu D_\mu \chi. \quad (1.5)$$

The gauge interaction¹ holds independently for

$$\Psi_L = \begin{pmatrix} 0 \\ \varphi \end{pmatrix} = \frac{1}{2}(\mathbb{1} - \gamma_5)\Psi \quad \text{and} \quad \Psi_R = \begin{pmatrix} \chi \\ 0 \end{pmatrix} = \frac{1}{2}(\mathbb{1} + \gamma_5)\Psi. \quad (1.6)$$

The Ψ_L and Ψ_R can transform differently under gauge transformations,

$$\Psi'_L = U_L \Psi_L \quad \text{and} \quad \Psi'_R = U_R \Psi_R. \quad (1.7)$$

But

$$m \bar{\Psi} \Psi = m(\varphi^\dagger, \chi^\dagger) \begin{pmatrix} \chi \\ \varphi \end{pmatrix} = m(\varphi^\dagger \chi + \chi^\dagger \varphi) = m(\bar{\Psi}_L \Psi_R + \bar{\Psi}_R \Psi_L). \quad (1.8)$$

The mass term mixes Ψ_L and Ψ_R . From this follows *symmetry breaking* if Ψ_L and Ψ_R transform differently.

What about the mass term for gauge bosons? We have the Lagrangian

$$\mathcal{L} = -\frac{1}{4} \underbrace{F^{\alpha\mu\nu} F_{\mu\nu}^\alpha}_{\text{gauge invariant}} + \frac{m^2}{2} \underbrace{A^{\alpha\mu} A_\mu^\alpha}_{\text{not gauge invariant}}. \quad (1.9)$$

For example for the $U(1)$ we get²

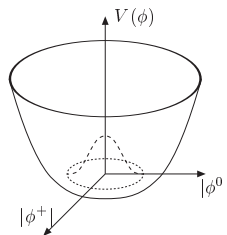
$$(A_\mu A^\mu)' = (A_\mu + \partial_\mu \theta)(A^\mu + \partial^\mu \theta) = A_\mu A^\mu + 2A_\mu \partial^\mu \theta + (\partial_\mu \theta)(\partial^\mu \theta). \quad (1.10)$$

The mass term A^μ breaks the gauge symmetry.

1.2 The Standard Model Higgs sector

The problem of mass generation without violating gauge symmetries can be solved by introducing an $SU(2)_L$ Higgs doublet³ with weak isospin $I = 1/2$ and hypercharge $Y = 1$ and the SM Higgs potential given by

$$V(\Phi) = \lambda \left[\Phi^\dagger \Phi - \frac{v^2}{2} \right]^2. \quad (1.11)$$



¹Question: What is the gauge principle?

²The kinetic Lagrangian $-1/4 F_{\mu\nu} F^{\mu\nu}$ is invariant under a gauge transformation $A_\mu \rightarrow A'_\mu = A_\mu + \partial_\mu \theta$.

³Question: Why do we need to introduce a doublet?

Here v denotes the vacuum expectation value (VEV)

$$v = \frac{1}{\sqrt{\sqrt{G_F}}} \approx 246.22 \text{ GeV}, \quad (1.12)$$



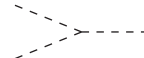

and $G_F = 1.16637 \cdot 10^{-5} \text{ GeV}^{-2}$ the Fermi constant. Introducing the Higgs field in a physical gauge,

$$\Phi = \frac{1}{\sqrt{2}} \begin{pmatrix} 0 \\ v + H \end{pmatrix}, \quad (1.13)$$

the Higgs potential can be written as

$$V(H) = \frac{1}{2} M_H^2 H^2 + \frac{M_H^2}{2v} H^3 + \frac{M_H^2}{8v^2} H^4. \quad (1.14)$$

Here we can read off directly the mass of the Higgs boson and the Higgs trilinear and quartic self-interactions. Adding the couplings to gauge bosons and fermions we have⁴:

Mass of the Higgs boson	$M_H = \sqrt{2\lambda}v$	
Couplings to gauge bosons	$g_{VVH} = \frac{2M_V^2}{v}$	
Yukawa couplings	$g_{ffH} = \frac{m_f}{v}$	
Trilinear coupling [units $\lambda_0 = 33.8 \text{ GeV}$]	$\lambda_{HHH} = 3 \frac{M_H^2}{M_Z^2}$	
Quartic coupling [units λ_0^2]	$\lambda_{HHHH} = 3 \frac{M_H^2}{M_Z^4}$	

In the SM the trilinear and quartic Higgs self-couplings are uniquely determined by the mass of the Higgs boson. As can be read off from the table, before the Higgs discovery the only unknown parameter was the Higgs boson mass.

The Higgs potential with its typical form leads to a non-vanishing VEV v in the ground state. Expansion of Φ around the minimum of the Higgs potential leads to one massive scalar particle, the Higgs boson, and three massless Goldstone bosons, that are absorbed to give masses to the charged W bosons and the Z boson. (For a toy example, see Appendix 3.1.) The appearance of Goldstone bosons is stated in the Goldstone theorem, which says:

Be

- N = dimension of the algebra of the symmetry group of the complete Lagrangian.
- M = dimension of the algebra of the group, under which the vacuum is invariant after spontaneous symmetry breaking.

\Rightarrow There are $N - M$ Goldstone bosons without mass in the theory.

The Goldstone theorem states that for each spontaneously broken degree of freedom of the symmetry there is one massless Goldstone boson.

In gauge theories, however, the conditions for the Goldstone theorem are not fulfilled: Massless scalar degrees of freedom are absorbed by the gauge bosons to give them mass. The Goldstone phenomenon leads to the Higgs phenomenon.

⁴The trilinear and quartic Higgs self-couplings are given in terms of $\lambda_0 = M_Z^2/v \approx 33.8 \text{ GeV}$.

1.3 Verification of the Higgs mechanism

On 4th July 2012, the LHC experiments ATLAS and CMS announced the discovery of a new scalar particle with mass $M_H \approx 125$ GeV [3, 4]. The discovery triggered immediately the investigation of the properties of this particle in order to test if it is indeed the Higgs particle that has been discovered. In order to verify experimentally the Higgs mechanism as the mechanism that allows to generate particle masses without violating gauge principles, we have to perform several steps:

- 1.) First of all the Higgs particle has to be discovered.
- 2.) In the next step its couplings to gauge bosons and fermions are measured. If the Higgs mechanism acts in nature these couplings are proportional to the masses (squared) of the respective particles.
- 3.) Its spin and parity quantum numbers have to be determined.
- 4.) And finally, the Higgs trilinear and quartic self-couplings must be measured. This way, the Higgs potential can be reconstructed which, with its typical minimax form, is responsible for the non-vanishing vacuum expectation value, that is essential for the non-zero particle masses.

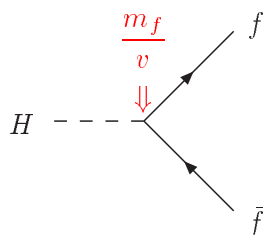
In the following, we will see how this program can be performed at the LHC.

1.4 Higgs boson decays

In order to search for the Higgs boson at existing and future colliders, one has to know what to look for. Hence, one has to study the Higgs decay channels. Since the Higgs boson couples proportional to the mass of the particle its preferred decays will be those into heavy particles, *i.e.* heavy fermions and, when kinematically allowed, into gauge bosons. The branching ratio into a final state pair XX is defined as

$$\text{BR}(H \rightarrow XX) = \frac{\Gamma(H \rightarrow XX)}{\Gamma_{\text{tot}}^H}. \quad (1.15)$$

The partial decay width for the decay $H \rightarrow XX$ is given by $\Gamma(H \rightarrow XX)$. The total decay width Γ_{tot}^H is the sum of all possible partial decay widths of H . All possible branching ratios hence have to add up to 1. For the SM Higgs boson of mass $M_H = 125.09$ GeV the branching ratios into fermions are



$$\begin{aligned}
BR(H \rightarrow b\bar{b}) &\lesssim 0.5797 \\
BR(H \rightarrow \tau^+\tau^-) &\lesssim 0.06244 \\
BR(H \rightarrow c\bar{c}) &\lesssim 0.02879 \\
BR(H \rightarrow t\bar{t}) &\lesssim 0 \quad (\text{kinematically closed})
\end{aligned} \tag{1.16}$$

These and the following branching ratios are obtained from the program `HDECAY` [5, 6]. It is a Fortran code for the computation of the branching ratios and total widths of the SM Higgs boson and also of the MSSM and 2HDM Higgs bosons. The decay widths include, where applicable, the state-of-the-art higher-order QCD and electroweak corrections. Furthermore, off-shell decays into heavy-quark, massive gauge boson, neutral Higgs pair as well as Higgs and gauge boson final states. The latter two decays do not exist in the SM Higgs sector but only in extended Higgs sectors with a larger Higgs spectrum. There are also other programs on the market for the computation of the SM Higgs decays, see [7, 8, 9] for an overview.

The tree-level partial decay width into fermions is given by

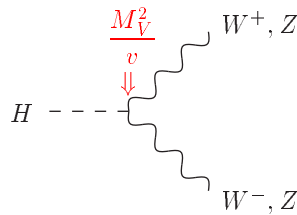
$$\Gamma(H \rightarrow f\bar{f}) = \frac{N_{cf}G_F M_H}{4\sqrt{2}\pi} m_f^2 \beta^3, \tag{1.17}$$

with the velocity

$$\beta = (1 - 4m_f^2/M_H^2)^{1/2} \tag{1.18}$$

of the fermions, their mass m_f , and the colour factor $N_{cf} = 1(3)$ for leptons (quarks). The decays into quark pair final states receive large QCD corrections which have been calculated by various groups and can amount up to -50%. [Braaten, Leveille; Sakai; Inami, Kubota; Drees, Hikasa; Gorishnii, Kataev, Larin, Surguladze; Kataev, Kim; Larin, van Ritbergen, Vermaseren; Chetyrkin, Kwiatkowski; Baikov, Chetyrkin, Kühn] - for details, see []].

For the SM Higgs boson with a mass of 125.09 GeV the branching ratios into gauge bosons are



$$\begin{aligned}
BR(H \rightarrow W^+W^-) &\lesssim 0.2167 \\
BR(H \rightarrow ZZ) &\lesssim 0.02657
\end{aligned} \tag{1.19}$$

For the 125 GeV Higgs boson these decays are off-shell, hence given by $H \rightarrow V^*V^* \rightarrow (f\bar{f})(f'\bar{f}')$ ($V = W, Z$). The Higgs boson decays into a pair of virtual vector bosons that subsequently decay into fermion pairs.

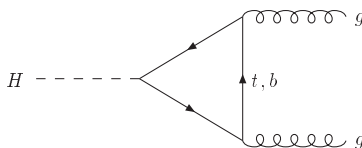
The formula for the tree-level decay width into a pair of on-shell massive gauge bosons $V = Z, W$ is given by

$$\Gamma(H \rightarrow VV) = \delta_V \frac{G_F M_H^3}{16\sqrt{2}\pi} \beta(1 - 4x + 12x^2), \tag{1.20}$$

with $x = M_V^2/M_H^2$, $\beta = \sqrt{1-4x}$ and $\delta_V = 2(1)$ for $V = W(Z)$. The electroweak corrections to these decays are of the order 5-20%.

[Fleischer, Jegerlehner; Bardin, ...; Kniehl; Ghinculov; Frink, ...] For a Higgs boson of mass $M_H = 125$ GeV off-shell decays $H \rightarrow V^*V^* \rightarrow 4l$ are important. The program PROPHECY4F includes the complete QCD and EW next-to-leading order (NLO) corrections to $H \rightarrow W^*W^*/Z^*Z^* \rightarrow 4f$ [Bredenstein, Denner; Dittmaier, Mück, Weber].

The decay into gluon pairs proceeds via a loop with the dominant contributions from top and bottom quarks:



For $M_H = 125.09$ GeV the branching ratio amounts to

$$BR(H \rightarrow gg) = 0.08157 . \quad (1.21)$$

At leading order (LO) the decay width can be cast into the form

$$\Gamma_{LO}(H \rightarrow gg) = \frac{G_F \alpha_s^2 M_H^3}{36\sqrt{2}\pi^3} \left| \sum_{Q=t,b} A_Q^H(\tau_Q) \right|^2 , \quad (1.22)$$

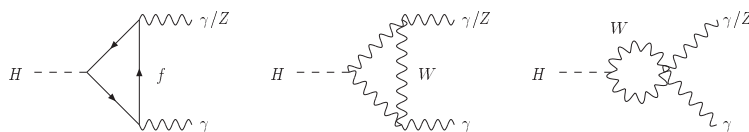
with the form factor

$$A_Q^H = \frac{3}{2}\tau[1 + (1 - \tau)f(\tau)] \quad (1.23)$$

$$f(\tau) = \begin{cases} \arcsin^2 \frac{1}{\sqrt{\tau}} & \tau \geq 1 \\ -\frac{1}{4} \left[\log \frac{1+\sqrt{1-\tau}}{1-\sqrt{1-\tau}} - i\pi \right]^2 & \tau < 1 \end{cases} . \quad (1.24)$$

The parameter $\tau_Q = 4M_Q^2/M_H^2$ is defined by the pole mass M_Q of the heavy quark Q in the loop. Note that for large quark masses the form factor approaches unity. The strong coupling constant is denoted by α_s . The QCD corrections have been calculated [Baikov, Chetyrkin; Chetyrkin, Kniehl, Steinhauser; Krämer, Laenen, Spira; Schröder, Steinhauser; Chetyrkin, Kühn, Sturm; Inami eal; Djouadi, Graudenz, Spira, Zerwas; Dawson eal; Harlander, Steinhauser; Harlander, Hofmann]. They are large and increase the branching ratio by about 70% at next-to-leading order (NLO). They are known at NLO including the full quark mass dependence and up to next-to-next-to-next-to leading order (N³LO) in the heavy top quark limit.

Further loop-mediated decays are those into 2 photons and a photon and a Z boson. They are mediated by charged fermion and W boson loops, the latter being dominant.



Although they amount only up to

$$BR(H \rightarrow \gamma\gamma) = 2.265 \times 10^{-3} \quad \text{and} \quad BR(H \rightarrow Z\gamma) = 1.537 \times 10^{-3} , \quad (1.25)$$

the $\gamma\gamma$ final state is an important search mode for light Higgs bosons at the LHC. The partial decay width into photons reads

$$\Gamma(H \rightarrow \gamma\gamma) = \frac{G_F \alpha^2 M_H^3}{128 \sqrt{2} \pi^3} \left| \sum_f N_{cf} e_f^2 A_f^H(\tau_f) + A_W^H(\tau_W) \right|^2, \quad (1.26)$$

with the form factors

$$A_f^H(\tau) = 2\tau[1 + (1 - \tau)f(\tau)] \quad (1.27)$$

$$A_W^H(\tau) = -[2 + 3\tau + 3\tau(2 - \tau)f(\tau)], \quad (1.28)$$

with the function $f(\tau)$ defined in Eq. (1.24). The parameters $\tau_i = 4M_i^2/M_H^2$ ($i = f, W$) are defined by the corresponding masses of the heavy loop particles. N_{cf} denotes again the colour factor of the fermion and e_f its electric charge. For large loop masses the form factors approach constant values,

$$\begin{aligned} A_f^H &\rightarrow \frac{4}{3} && \text{for } M_H^2 \ll 4M_Q^2 \\ A_W^H &\rightarrow -7 && \text{for } M_H^2 \ll 4M_W^2. \end{aligned} \quad (1.29)$$

The W loop provides the dominant contribution in the intermediate Higgs mass regime, and the fermion loops interfere destructively. The QCD corrections have been calculated and are small in the intermediate Higgs boson mass region. [Zheng, Wu; Djouadi, Graudenz Spira, Zerwas; Melnikov, Spira, Yakovlev; Dawson, Kauffmann; Melnikov, Yakovlev; Inoue, Najima, Okada, Saito] The tree-level decay width into $Z\gamma$ is given

$$\Gamma(H \rightarrow Z\gamma) = \frac{G_F^2 M_W^2 \alpha M_H^3}{64\pi^4} \left(1 - \frac{M_Z^2}{M_H^2}\right)^3 \left| \sum_f A_f^H(\tau_f, \lambda_f) + A_W^H(\tau_W, \lambda_W) \right|^2, \quad (1.30)$$

with the form factors

$$\begin{aligned} A_f^H(\tau, \lambda) &= 2N_{cf} \frac{e_f(I_{3f} - 2e_f \sin^2 \theta_W)}{\cos \theta_W} [I_1(\tau, \lambda) - I_2(\tau, \lambda)] \\ A_W^H(\tau, \lambda) &= \cos \theta_W \left\{ 4(3 - \tan^2 \theta_W) I_2(\tau, \lambda) \right. \\ &\quad \left. + \left[\left(1 + \frac{2}{\tau}\right) \tan^2 \theta_W - \left(5 + \frac{2}{\tau}\right) \right] I_1(\tau, \lambda) \right\}. \end{aligned} \quad (1.31)$$

The functions I_1 and I_2 read

$$I_1(\tau, \lambda) = \frac{\tau\lambda}{2(\tau - \lambda)} + \frac{\tau^2\lambda^2}{2(\tau - \lambda)^2} [f(\tau) - f(\lambda)] + \frac{\tau^2\lambda}{(\tau - \lambda)^2} [g(\tau) - g(\lambda)] \quad (1.32)$$

$$I_2(\tau, \lambda) = -\frac{\tau\lambda}{2(\tau - \lambda)} [f(\tau) - f(\lambda)]. \quad (1.33)$$

The function $g(\tau)$ can be cast into the form

$$g(\tau) = \begin{cases} \sqrt{\tau - 1} \arcsin \frac{1}{\sqrt{\tau}} & \tau \geq 1 \\ \frac{\sqrt{1-\tau}}{2} \left[\log \frac{1+\sqrt{1-\tau}}{1-\sqrt{1-\tau}} - i\pi \right] & \tau < 1 \end{cases} \quad (1.34)$$

The parameters $\tau_i = 4M_i^2/M_H^2$ and $\lambda_i = 4M_i^2/M_Z^2$ ($i = f, W$) are defined in terms of the corresponding masses of the heavy loop particles. The W loop dominates in the intermediate Higgs mass range, and the heavy fermion loops interfere destructively.

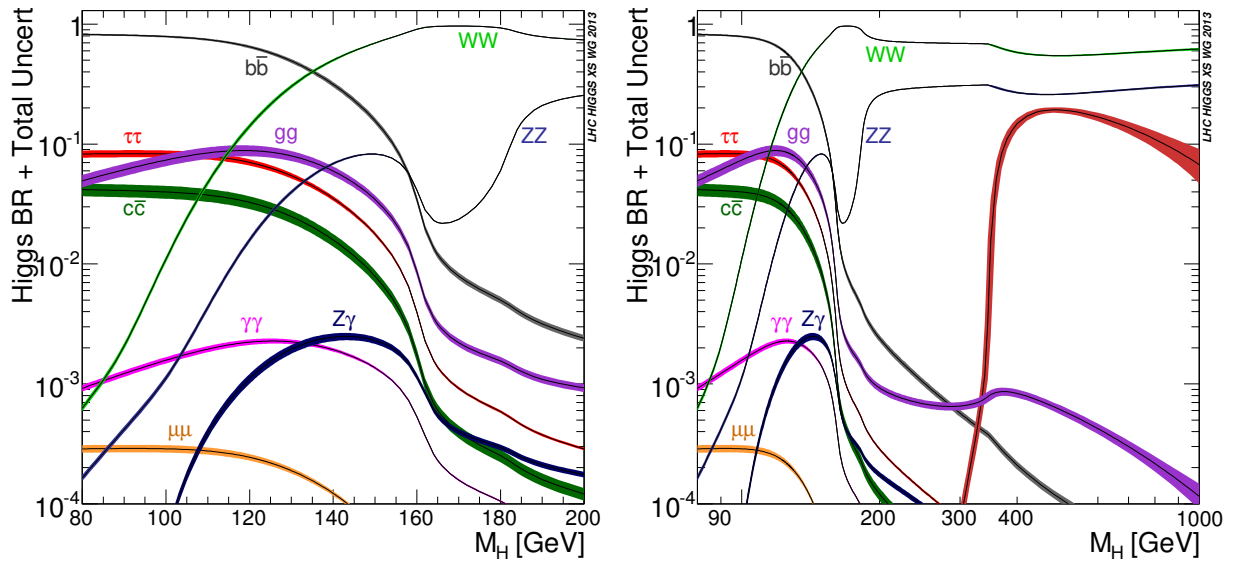


Figure 1.2: The Higgs boson branching ratios as a function of the Higgs boson mass: zoomed in low-mass region (left), whole canonical mass region (right). Plot taken from the LHC Higgs Cross Section Working Group Report 3 [8].

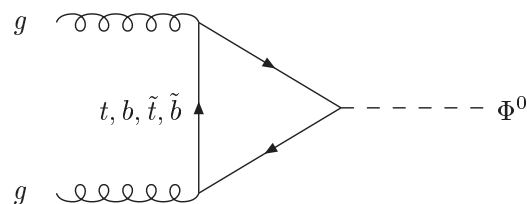
Figs. 1.2 and 1.3 show plots as they were already produced before the Higgs boson discovery when the Higgs boson mass was still unknown. Shown are the Higgs boson branching ratios and total width, respectively, as a function of the Higgs boson mass. One can infer from the figures that the total Higgs boson width is rather small, less than ~ 10 MeV, for masses below about 140 GeV. Once the threshold for gauge boson decays is reached the total width increases rapidly up to about 600 GeV for $M_H = 1$ TeV. The gauge boson decay widths are proportional to M_H^3 . Below the gauge boson threshold the main decay is into $b\bar{b}$, followed by the decay into $\tau^+\tau^-$. - The error bands include the parametric and theoretical uncertainties.

1.5 Higgs boson production at the LHC

There are several Higgs boson production mechanisms at the LHC.

- Gluon fusion: The dominant production mechanism for Standard Model Higgs bosons at the LHC is gluon fusion

[Georgi, et al.;Gamberini, et al.]



$$pp \rightarrow gg \rightarrow H .$$

$$(1.35)$$

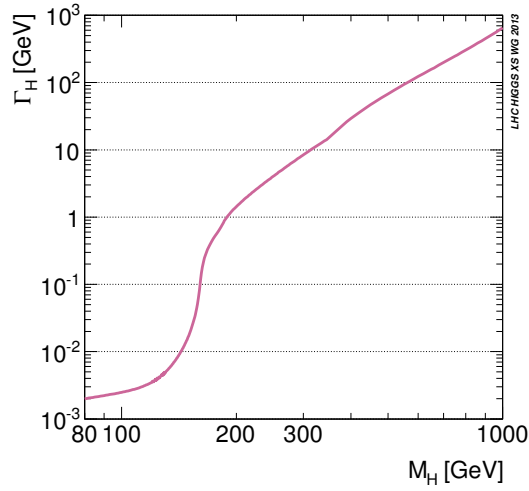


Figure 1.3: The Higgs boson total width as a function of the Higgs boson mass. Plot taken from the LHC Higgs Cross Section Working Group Report 3 [8].

In the Standard Model it is mediated by top and bottom quark loops. The QCD corrections (the next-to leading order calculation involves 2-loop diagrams!) have been calculated and turn out to be large. They are of the order 10-100%. [Spira, Djouadi, Graudenz, Zerwas; Dawson, Kauffmann, Schaffer]; see Fig. 1.4, which shows the NLO K -factor, *i.e.* the ratio of the NLO cross section to the leading order (LO) cross section as a function of the Higgs boson mass for the virtual and real corrections.

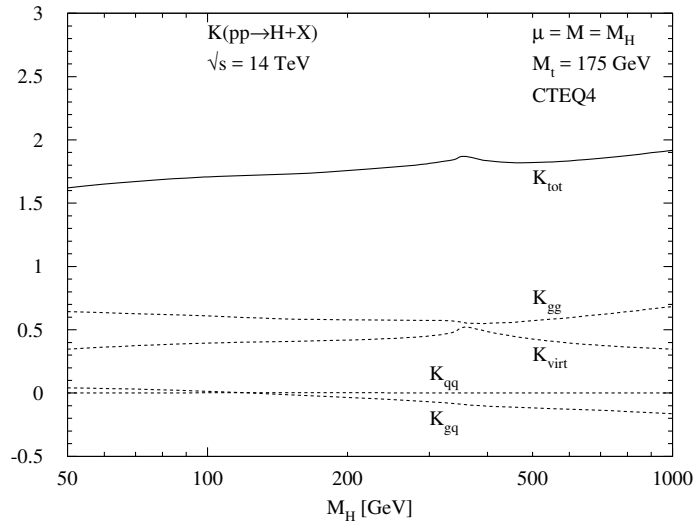


Figure 1.4: The K factor for the gluon fusion process as a function of the Higgs boson mass.

Due to the inclusion of the NLO QCD corrections the scale dependence of the gluon fusion cross section is decreased, *cf.* Fig. 1.5.

The next-to-next-to leading order (NNLO) corrections have been calculated in the limit of heavy top quark masses ($M_H \ll m_t$) [Harlander,Kilgore;Anastasiou,Melnikov;Ravindran,...].

They lead to a further increase of the cross section by 20-30%. The scale dependence is reduced to $\Delta \lesssim 10 - 15\%$. Resummation of the soft gluons [Catani, et al.; ...] adds another 10%. There has been a lot of progress in the computation of the higher-order corrections to

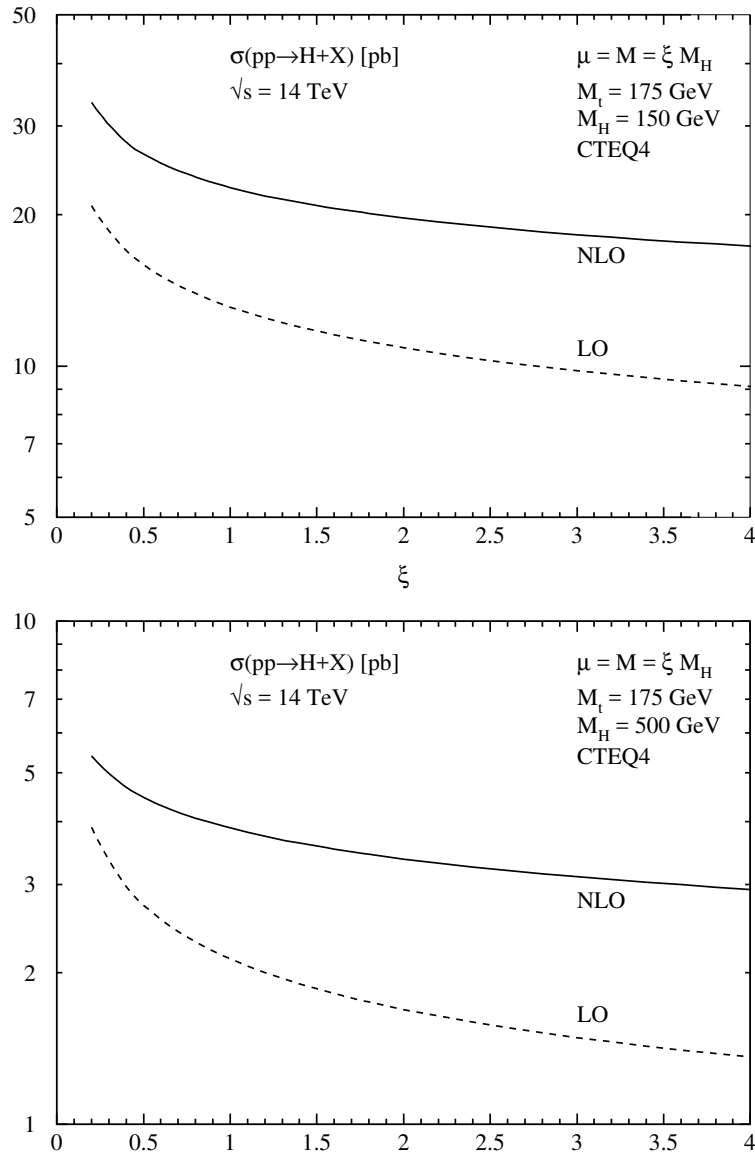


Figure 1.5: The scale dependence of the gluon fusion cross section for two different Higgs boson masses.

gluon fusion in the last years.

Status of higher order (HO) corrections:

- ▷ complete NLO: increase σ by $\sim 10-100\%$
- ▷ SM: limit $M_\Phi \ll m_t$ - approximation $\sim 20-30\%$
- ▷ NNLO @ $M_\Phi \ll m_t \Rightarrow$ further increase by 20-30%

top mass effects are small in the SM

- ▷ NNNLO for $M_\Phi \ll m_t \rightsquigarrow$ scale stabilisation

scale dependence: $\Delta \lesssim 5\%$

- ▷ NNNLL soft resummation: $\sim 2\%$
- ▷ leading soft contribution at N³LO in limit $m_t \rightarrow \infty$
- ▷ SM+2HDM EW corrections $\sim 5\%$
- ▷ impl. in POWHEG including mass effects at NLO

Spira,Djouadi,Graudenz,Zerwas
Dawson;Kauffman,Schaffer

Krämer,Laenen,Spira

Harlander,Kilgore

Anastasiou,Melnikov

Ravindran,Smith,van Neerven

Marzani,Ball,Del Duca,Forte,Vicini

Harlander,Ozeren

Pak,Rogal,Steinhauser

Moch,Vogt

Ravindran

de Florian,Mazzitelli,Moch,Vogt

Anastasiou,Duhr,Dulat,Furlan,Gehrmann,Herzog,Mistlberger

Ball,Bonvini,Forte,Marzani,Ridolfi

Catani,de Florian,Grazzini,Nason

Ravindran

Ahrens,Becher,Neubert,Yang

Ball,Bonvini,Forte,Marzani,Ridolfi

Bonvini,Marzani

Schmidt,Spira

Ravindran,Smith,van Neerven; Ahrens eal

Aglietti eal

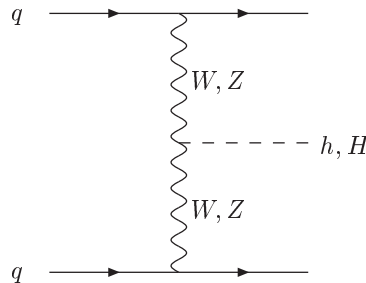
Degrassi,Maltoni

Actis,Passarino,Sturm,Uccirati

Jennis,Sturm,Uccirati

Bagnaschi,Degrassi,Slavich,Vicini

- WW/ZZ fusion: Higgs bosons can be produced in the WW/ZZ fusion processes [Cahn, Dawson; Hikasa; Altarelli, Mele, Pitolli]

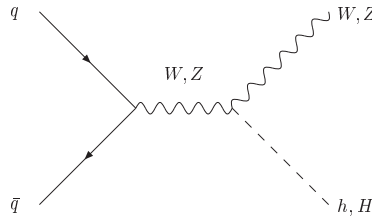


$$pp \rightarrow W^*W^*/Z^*Z^* \rightarrow H . \quad (1.36)$$

The QCD corrections have been calculated long time ago and amount up to $\sim 10\%$ [Han, Valencia, Willenbrock], [Figy,Oleary,Zeppenfeld], [Berger,Campbell]. In the meantime more higher-order QCD and EW corrections have been calculated.

- ▷ approximate 2-loop QCD corr. $\Rightarrow \lesssim 1\%$ Bolzano,Maltoni,Moch,Zaro
Cacciari,Dreyer,Karlberg,Salam,Zanderighi
- ▷ approximate 3-loop QCD corr. $\Rightarrow \lesssim 0.3\%$ Dreyer,Karlberg
- ▷ electroweak corr. $\Rightarrow \sim 10\%$ Ciccolini,Denner,Dittmaier

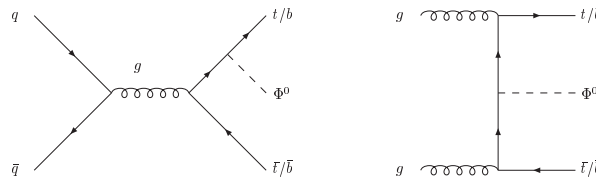
- Higgs-strahlung: Higgs boson production in Higgs-strahlung [Glashow et al.; Kunszt et al.] proceeds via



$$pp \rightarrow W^*/Z^* \rightarrow W/Z + H . \quad (1.37)$$

The QCD corrections are $\sim 30\%$ [Han,Willenbrock]. The NNLO QCD corrections add another $\lesssim 5\%$ [Harlander, Kilgore; Hamberg, Van Neerven, Matsuura; Brein, Djouadi, Harlander]. The theoretical error is reduced to about 5%. The complete electroweak (EW) corrections reduce the cross section by 5-10% [Ciccolini, Dittmaier, Krämer]. Furthermore, the $W/Z + H$ production has been provided fully exclusively at NNLO QCD [Ferrera,Grazzini,Tramantano].

- Associated Production: Higgs bosons can also be produced in association with top and bottom quarks [Kunszt; Gunion; Marcano, Paige]



$$pp \rightarrow t\bar{t}/b\bar{b} + H . \quad (1.38)$$

The process $t\bar{t}H \rightarrow t\bar{t}b\bar{b}$ is important at the LHC as it gives access to the top Yukawa coupling. The NLO QCD corrections to associated top production increase the cross section at the LHC by 20% [Beenakker, et al.; Dawson, et al.]. The parton level cross section has been linked to parton showers in the tools `aMC@NLO` and `PowHel` [Frederix et al.; Garzelli,Kardos,Papadopoulos,Trocsanyi]. There has been important work on the background $t\bar{t}b\bar{b}, t\bar{t}jj$ etc. [Bredenstein,Denner,Dittmaier,Pozzorini; Bevilacqua,Czakon,Papadopoulos,Pittau,Worek; Cascioli,Maierhofer,Pozzorini] Fig. 1.5 shows the production cross sections in pb as a function of the Higgs boson mass. The bands show the residual theoretical error.

1.6 Higgs Boson Discovery

The main Higgs discovery channels are the $\gamma\gamma$ and Z^*Z^* final states. The decay into $\gamma\gamma$ final states has a very small branching ratio, but is very clean. (CMS and ATLAS have an excellent photon-energy resolution. Look for narrow $\gamma\gamma$ invariant mass peak, extrapolate background into the signal region from thresholds.). The Z^*Z^* final state is the other important search channel. For $M_H = 125$ GeV it is an off-shell decay. It leads to a clean 4 lepton (4l) final state from the decay of the Z bosons. Also the WW final state is off-shell. The final state signature includes missing energy from the neutrinos of the W boson decays. The $b\bar{b}$ final state is exploited as well. It has the largest branching ratio, but suffers from a large QCD

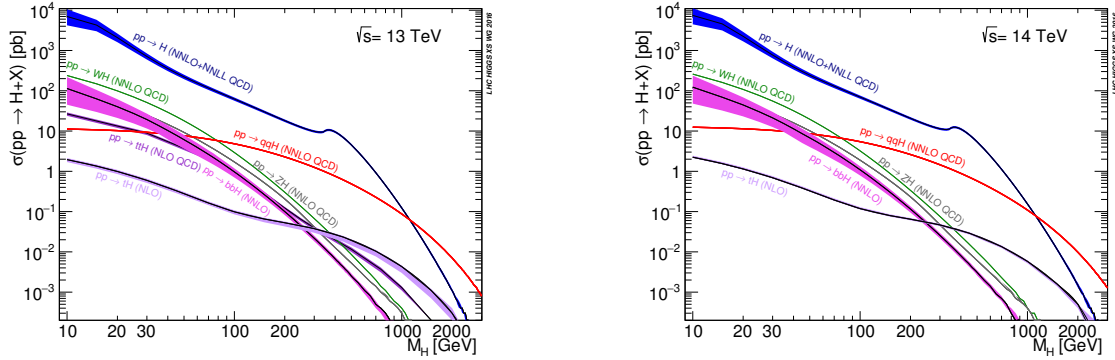


Figure 1.6: The Higgs boson production cross sections at the LHC as a function of the Higgs boson mass for a center-of-mass energy of 13 TeV (left) and 14 TeV (right).

background. Finally, the $\tau\tau$ channel is also used.

The main discovery channels for the 125 GeV Higgs boson at ATLAS and CMS, *i.e.* the photon and the Z boson final states, are shown in Fig. 1.7.

The experiments give the best fit values to the reduced μ values in the final state X . These are the production rate times branching ratio into the final state $X = \gamma, Z, W, b, \tau$ normalized to the corresponding value for a SM Higgs boson,

$$\mu = \frac{\sigma_{\text{prod}} \times BR(H \rightarrow XX)}{(\sigma_{\text{prod}} \times BR(H \rightarrow XX))_{\text{SM}}} . \quad (1.39)$$

In case the discovered Higgs boson is a SM Higgs boson they are all equal to 1. Figure 1.8 shows the μ values reported by the LHC experiments. The various final states suffer from uncertainties that leave room for beyond the SM (BSM) physics.

1.7 Higgs boson couplings at the LHC

In principle the strategy to measure the Higgs boson couplings is to combine various Higgs production and decay channels, from which the couplings can then be extracted. For example, the production of the Higgs boson in W boson fusion with subsequent decay into τ leptons, Fig. 1.9, is proportional to the partial width into WW and the branching ratio into $\tau\tau$. Combination with other production/decay channels and the knowledge of the total width allow then to extract the Higgs couplings. The problem at the LHC, however, is that the total width, which is small for a SM 125 GeV Higgs boson, cannot be measured without model-assumptions, and also not all final states are accessible experimentally. Therefore without applying model-assumptions only ratios of couplings are measurable.

The theoretical approach is to define an effective Lagrangian with modified Higgs couplings. In a first approach the couplings are modified by overall scale factors κ_i and the tensor structure is not changed. With this Lagrangian the signal rates, respectively μ values, are calculated as function of the scaling factors, $\mu(\kappa_i)$. These are then fitted to the experimentally measured μ values. The fits provide then the κ_i values. Such a theoretical

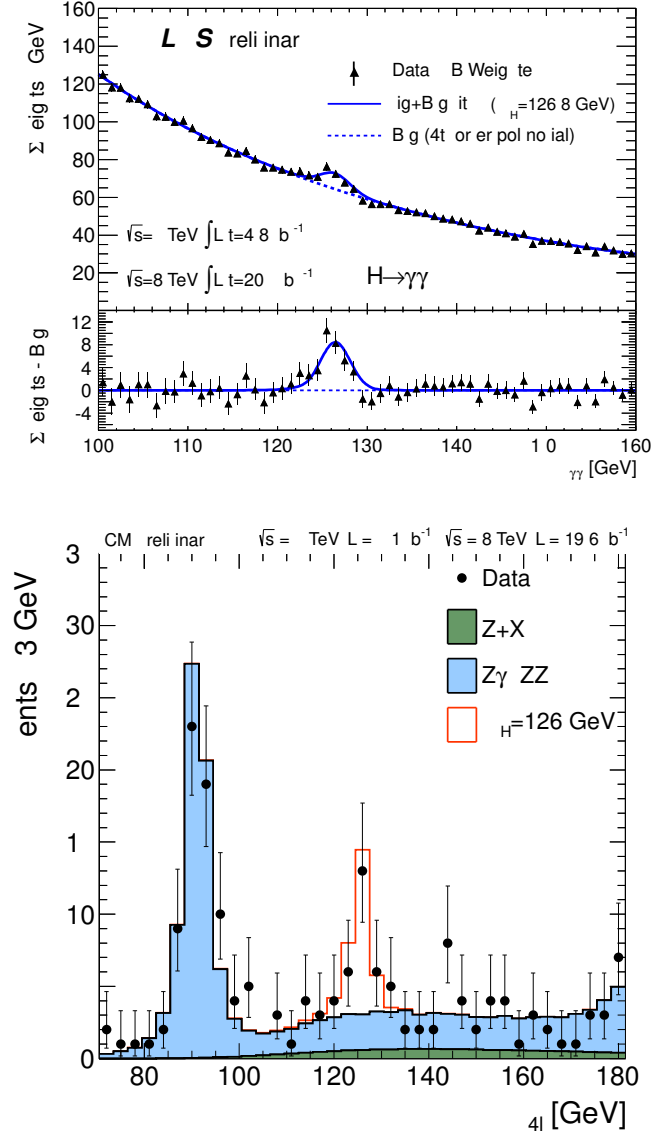


Figure 1.7: The main Higgs discovery channels: Upper: The photon final state, here shown for the ATLAS experiment [ATLAS-CONF-2013-12]. Lower: The Z^*Z^* final state, here shown for the CMS experiment [CMS-PAS-HIG-13-002].

Lagrangian for the SM field content with a scalar particle h looks like

$$\begin{aligned} \mathcal{L} = & \mathcal{L}_h - (M_W^2 W_\mu^+ W^{\mu-} + \frac{1}{2} M_Z^2 Z_\mu Z^\mu) [1 + 2\kappa_V \frac{h}{v} + \mathcal{O}(h^2)] \\ & - m_{\psi_i} \bar{\psi}_i \psi_i [1 + \kappa_F \frac{h}{v} + \mathcal{O}(h^2)] + \dots \end{aligned} \quad (1.40)$$

It is valid below the scale Λ where new physics (NP) becomes important. It implements the electroweak symmetry breaking (EWSB) via \mathcal{L}_h and the custodial symmetry through $\kappa_W = \kappa_Z = \kappa_V$. Furthermore, there are no tree-level flavour changing neutral current (FCNC) couplings as κ_F is chosen to be the same for all fermion generations and does not allow for transitions between fermion generations. The best fit values for κ_f and κ_V are

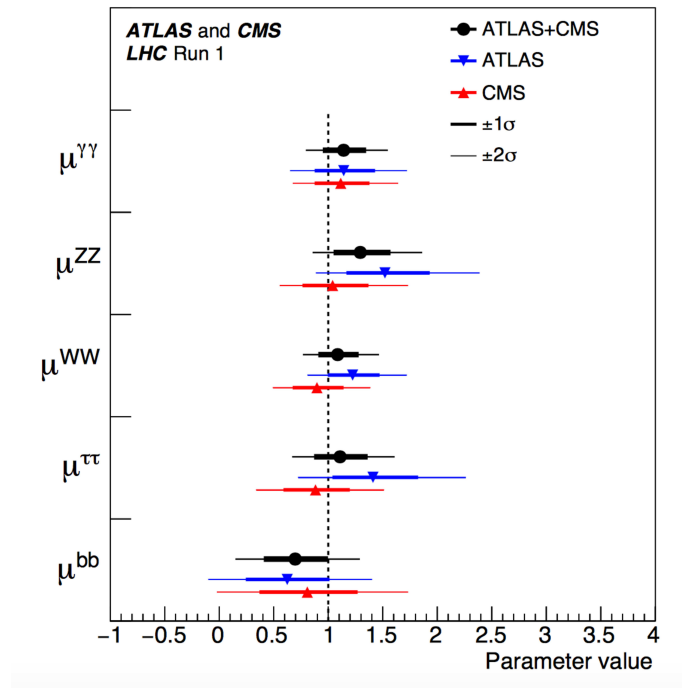


Figure 1.8: Combined best fits for the μ values from the ATLAS and CMS experiments based on Run 1 data.

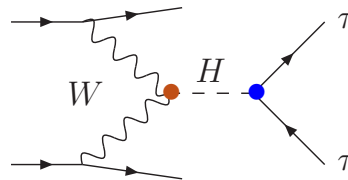


Figure 1.9: Feynman diagram for the production of a Higgs boson in W boson fusion with subsequent decay into $\tau\tau$. It is proportional to the partial width Γ_{WW} and the branching ratio into $\tau\tau$, $\text{BR}(H \rightarrow \tau\tau)$.

shown in Fig. 1.10.

If the discovered particle is the Higgs boson the coupling strengths are proportional to the masses (squared) of the particles to which the Higgs boson couples. This trend can be seen in the plot published by CMS, see Fig. 1.11.

1.8 Higgs Boson Quantum Numbers

The Higgs boson quantum numbers can be extracted by looking at the threshold distributions and the angular distributions of various production and decay processes. The SM Higgs

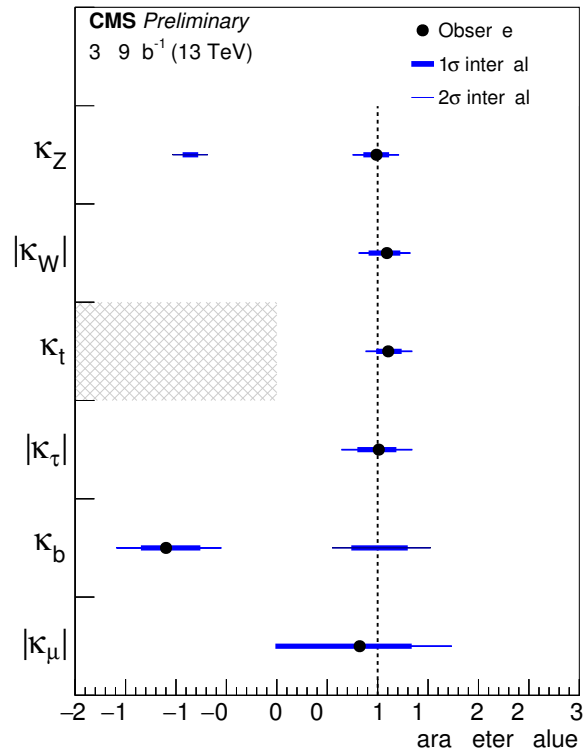
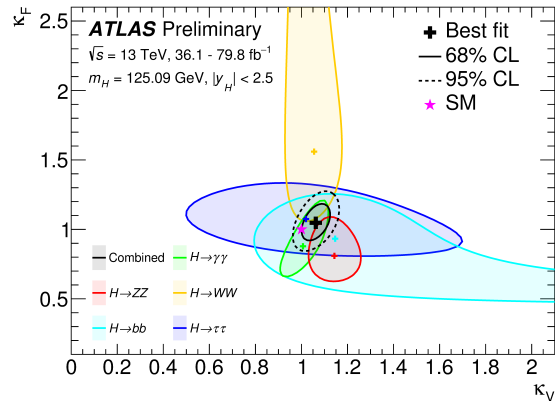


Figure 1.10: The best fit values for κ_f and κ_V by ATLAS (upper). The best fit values to the κ 's measured by CMS [CMS-PAS-HIG-17-031] (lower).

boson has spin 0, positive parity P and is even under charge conjugation C . From the observation of the Higgs boson in the $\gamma\gamma$ final state one can already conclude that it does not have spin 1, due to the Landau-Yang theorem, and that it has $C = +1$, assuming charge invariance. However, these are theoretical considerations and have to be proven also experimentally.

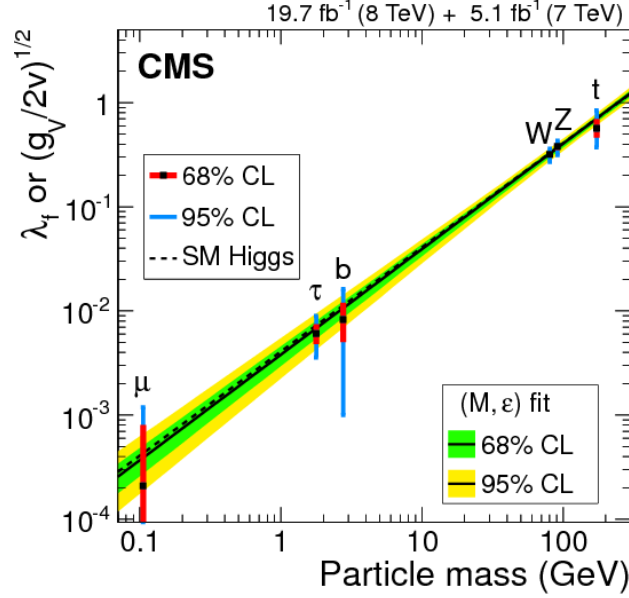


Figure 1.11: Coupling strengths as function of the mass of the particles coupled to the Higgs boson.

The theoretical tools to provide angular distributions for a particle with arbitrary spin and parity are helicity analyses and operator expansion. Let us look as an example at the Higgs decay into ZZ^* , and the Z bosons subsequently decay into 4 leptons,

$$H \rightarrow ZZ^{(*)} \rightarrow (f_1\bar{f}_1)(f_2\bar{f}_2). \quad (1.41)$$

The decay is illustrated in Fig. 1.12. The angle φ is the azimuthal angle between the decay planes of the Z bosons in the H rest frame. The θ_1 and θ_2 are the polar angles, respectively, of the fermion pairs in, respectively, the rest frame of the decaying Z boson.

For the SM the double polar angle distribution reads

$$\frac{1}{\Gamma'} \frac{d\Gamma'}{d\cos\theta_1 d\cos\theta_2} = \frac{9}{16} \frac{1}{\gamma^4 + 2} \left[\gamma^4 \sin^2\theta_1 \sin^2\theta_2 + \frac{1}{2} (1 + \cos^2\theta_1)(1 + \cos^2\theta_2) \right] \quad (1.42)$$

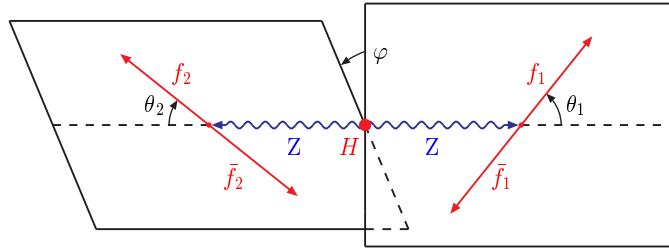
and the azimuthal angular distribution is given by

$$\frac{1}{\Gamma'} \frac{d\Gamma'}{d\phi} = \frac{1}{2\pi} \left[1 + \frac{1}{2} \frac{1}{\gamma^4 + 2} \cos 2\phi \right] \quad (1.43)$$

The verification of these distributions is a necessary step for the proof of the 0^+ nature of the Higgs boson.

The calculation of the azimuthal angular distribution delivers a different behaviour for a scalar and a pseudoscalar boson:

$$\begin{aligned} 0^+ &: d\Gamma/d\phi \sim 1 + 1/(2\gamma^4 + 4) \cos 2\phi \\ 0^- &: d\Gamma/d\phi \sim 1 - 1/4 \cos 2\phi \end{aligned} \quad (1.44)$$

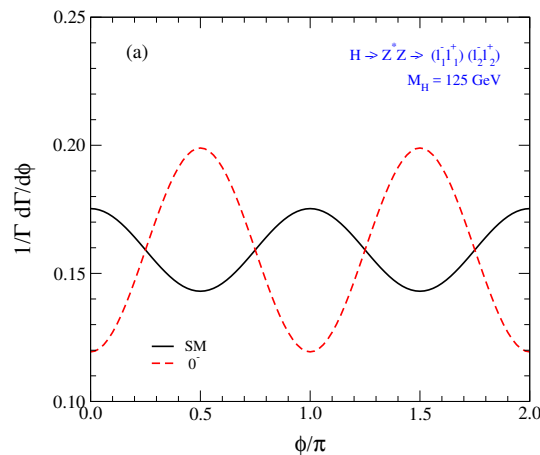

 Figure 1.12: The decay $H \rightarrow ZZ^* \rightarrow (f_1 \bar{f}_1)(f_2 \bar{f}_2)$.

Here $\gamma^2 = (M_H^2 - M_*^2 - M_Z^2)/(2M_*M_Z)$ and M_* is the mass of the virtual Z boson. Figure 1.13 shows how the azimuthal angular distribution can be exploited to test the parity of the particle. A pseudoscalar with spin-parity 0^- shows the opposite behaviour in this distribution than the scalar, which is due to the minus sign in front of $\cos 2\phi$ in Eq. (1.44). The threshold behaviour on the other hand can be used to determine the spin of the particle. We have for spin 0 a linear rise with the velocity β ,

$$\frac{d\Gamma[H \rightarrow Z^*Z]}{dM_*^2} \sim \beta = \sqrt{(M_H - M_Z)^2 - M_*^2}/M_H. \quad (1.45)$$

A spin 2 particle, *e.g.* shows a flatter rise, $\sim \beta^3$, *cf.* Fig. 1.14.

The experiments cannot perform an independent spin-parity measurement. Instead they test various spin-parity hypotheses. Various non-SM spin-parity hypotheses have been ruled out at more than 95% confidence level (C.L.), see *e.g.* Fig. 1.15.


 Figure 1.13: The azimuthal distribution for the $H \rightarrow ZZ^* \rightarrow 4l$ decay for the SM scalar Higgs (black) and a pseudoscalar (red). [Choi,Mühlleitner,Zerwas]

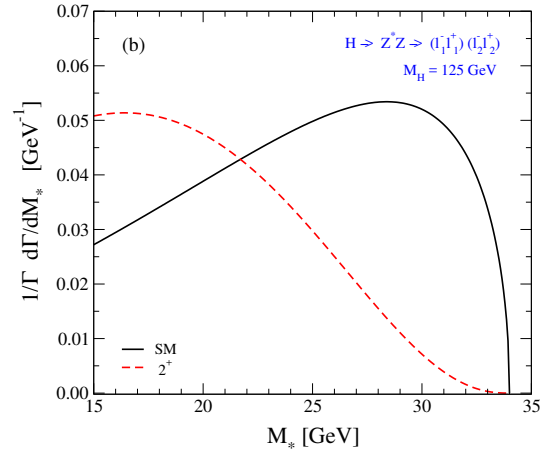


Figure 1.14: The threshold distribution for the $H \rightarrow ZZ^* \rightarrow 4l$ decay for the SM spin-0 Higgs (black) and a spin-2 particle (red).[Choi,Mühlleitner,Zerwas]

1.9 Determination of the Higgs self-interactions

In order to fully establish the Higgs mechanism as the one responsible for the generation of particle masses without violating gauge principles, the Higgs potential has to be reconstructed. This can be done once the Higgs trilinear and quartic self-interactions have been measured. The trilinear coupling λ_{HHH} is accessible in double Higgs production. The quartic coupling λ_{HHHH} is to be obtained from triple Higgs production.

1.9.1 Determination of the Higgs self-couplings at the LHC

The processes for the extraction of λ_{HHH} [Djouadi,Kilian,Mühlleitner,Zerwas] at the LHC are gluon fusion into a Higgs pair, double Higgs-strahlung, WW/ZZ fusion and radiation of a Higgs pair off top quarks.

$$\begin{array}{llll}
 \text{gluon fusion:} & gg & \rightarrow & HH \\
 \text{double Higgs-strahlung:} & q\bar{q} & \rightarrow & W^*/Z^* \rightarrow W/Z + HH \\
 \text{WW/ZZ double Higgs fusion:} & qq & \rightarrow & qq + WW/ZZ \rightarrow HH \\
 \text{associated production:} & pp & \rightarrow & t\bar{t}HH
 \end{array} \tag{1.46}$$

The dominant gluon fusion production process proceeds via triangle and box diagrams, see Fig. 1.16.

Due to smallness of the cross sections, *cf.* Fig. 1.17, and the large QCD background the extraction of the Higgs self-coupling at the LHC is extremely difficult. There is an enormous theoretical activity to determine the production processes with high accuracy including HO corrections and to develop strategies and observables for the measurement of the di-Higgs production processes and the trilinear Higgs self-couplings. Status of higher order (HO) corrections:

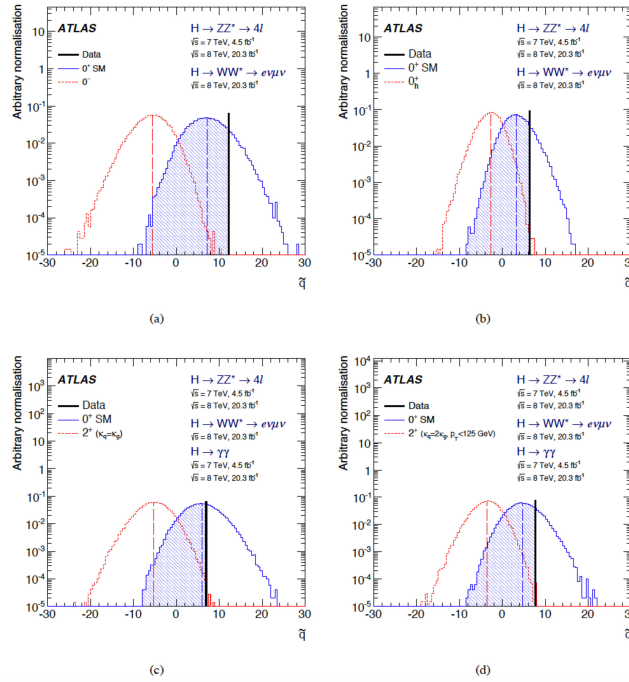


Figure 1.15: Examples of distributions of the test statistic \tilde{q} for the combination of decay channels. (a): 0^+ versus 0 ; (b): 0^+ versus 0_h^+ ; (c): 0^+ versus the spin-2 model with universal couplings ($\kappa_q = \kappa_g$); (d): 0^+ versus the spin-2 model with $\kappa_q = 2\kappa_g$ and the p_T selection at 125 GeV. The observed values are indicated by the vertical solid line and the expected medians by the dashed lines. The shaded areas correspond to the integrals of the expected distributions used to compute the p -values for the rejection of each hypothesis. Figure taken from and details in Eur. Phys. J. C75 (2015) no.10, 476, Erratum: Eur. Phys. J. C76 (2016) no.3, 152.

- ▷ LO cxn known exactly with full mass dependence
 - ▷ NLO QCD corrections - multi-scale problem
 - ▷ improved LET: $K = \sigma_{\text{NLO}}/\sigma_{\text{LO}} \sim 1.7$
 - ▷ Estimate of finite mass effects: inclusion of higher-order corr. in large m_t exp. $\mathcal{O}(\pm 10\%)$
 - ▷ real contribution w/ full m_t dependence \rightsquigarrow top mass effects: $\mathcal{O}(-10\%)$
 - ▷ Full NLO calculation \rightsquigarrow top mass effects: -14%
 - ▷ NNLO QCD corr. for expansion in small external momenta: $\mathcal{O}(20\%)$
 - ▷ threshold resumm., further increase NNLO+NNLL in large top mass limit NLL w/ top quark mass effects
 - ▷ Theoretical uncertainty: scale 6%, pdf 2%, α_s 2%
- Glover, van der Bij '88;
 Plehn, Spira, Zerwas '95

 Dawson, Dittmaier, Spira '98
 Grigo, Hoff, Melnikov, Steinhauser '13;
 Grigo, Hoff, Steinhauser '15;
 Degrossi, Giardino, Gröber '16

 Frederix, Frixione, Hirschi,
 Maltoni, Mattelaer, Torrielli,
 Vryonidou, Zaro '14

 Borowka et al '16
 de Florian, Mazzitelli '13 '15;
 Grigo, Melnikov, Steinhauser '14;
 Grigo, Hoff, Steinhauser '15;
 de Florian, Grazzini, Hanga, Kallweit,
 Lindert, Maierhöfer, Mazzitelli, Rathlev '16

 de Florian, Mazzitelli '15
 Ferrara, Pires '16

 LHC Higgs Cross Section WG

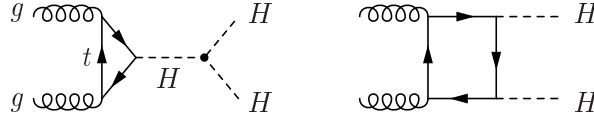


Figure 1.16: The diagrams that contribute to the gluon fusion process $gg \rightarrow HH$.

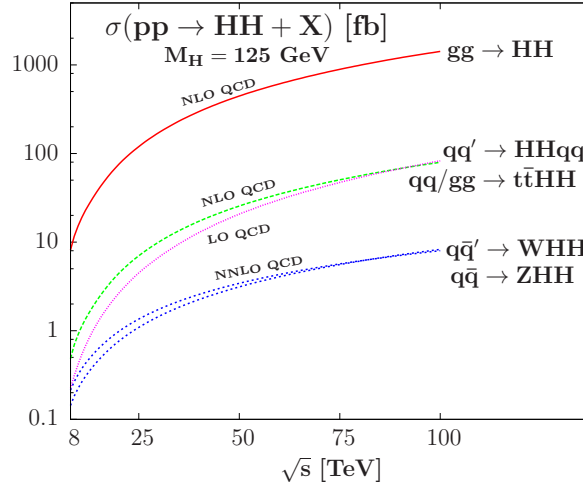


Figure 1.17: Di-Higgs production processes at the LHC with c.m. energy 14 TeV, including higher-order corrections. [Baglio,Djouadi,Gröber,Mühlleitner,Quévillon,Spira].

The next-to-leading order cross section for Higgs pair production at a c.m. energy of 14 TeV amounts to [Borowka eal '16]

$$\sigma_{gg \rightarrow HH}^{\text{NLO}} = 32.91_{-12.6\%}^{+13.6\%} \text{ fb} . \quad (1.47)$$

The current constraints on the SM trilinear Higgs self-coupling are [arXiv:1506.0028, 1509.0467, 1603.0689; ATLAS-CONF-2016-049] $\mathcal{O}(\pm 15 \lambda_{hhh}^{\text{SM}})$, *cf.* Fig. 1.18. The prospects in the $b\bar{b}\gamma\gamma$ final state are [ATL-PHYS-PUB-2017-001] $-0.8 < \lambda_{hh}/\lambda_{hhh}^{\text{SM}} < 7.7$.

1.10 Summary

The measurements of the properties of the discovered particle have identified it as the Higgs boson. CERN therefore officially announced in a press release of March 2013 that the discovered particle is the Higgs boson, *cf.* Fig. 1.19. This lead then to the Nobel Prize for Physics in 2013 to Francois Englert and Peter Higgs.

The SM of particle physics has been very successful so far. At the experiments it has been tested to highest accuracy, including higher order corrections. And with the discovery of the Higgs particle we have found the last missing piece of the SM of particle physics. Still there are many open questions that cannot be answered by the SM. To name a few of them

1. In the SM the Higgs mechanism is introduced ad hoc. There is no dynamical mechanism behind it.

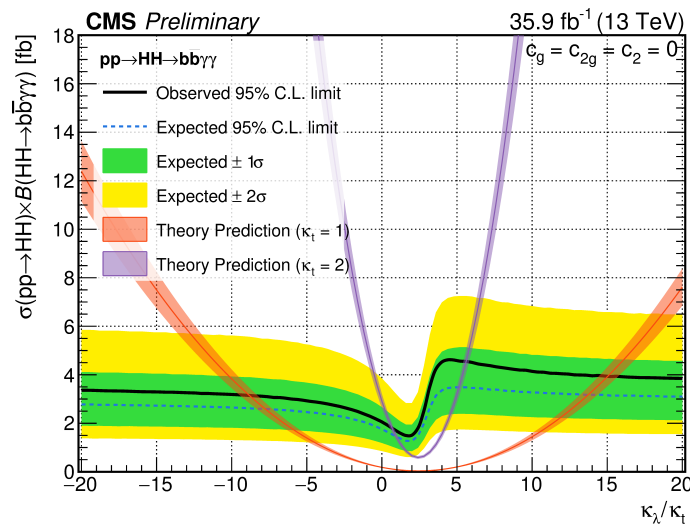


Figure 1.18: Plot taken from CMS-PAS-HIG-17-008.

2. In the presence of high energy scales, the Higgs boson mass receives large quantum corrections, inducing the hierarchy problem.
3. We have no explanation for the fermion masses and mixings.
4. The SM does not contain a Dark Matter candidate.
5. In the SM the gauge couplings do not unify.
6. The SM does not incorporate gravity.
7. The CP violation in the SM is not large enough to allow for baryogenesis.
8. ...

We therefore should rather see the SM as an effective low-energy theory which is embedded in some more fundamental theory that becomes apparent at higher scales. The Higgs data so far, although pointing towards a SM Higgs boson, still allow for interpretations within theories beyond the SM. These BSM theories can solve some of the problems of the SM. A few of these BSM models shall be presented in this lecture.

CERN press office

[Media visits](#) [Press releases](#) [For journalists](#) [For CERN people](#) [Contact us](#)

New results indicate that particle discovered at CERN is a Higgs boson

14 Mar 2013

Geneva, 14 March 2013. At the Moriond Conference today, the ATLAS and CMS collaborations at CERN¹'s Large Hadron Collider (LHC) presented preliminary new results that further elucidate the particle discovered last year. Having analysed two and a half times more data than was available for the discovery announcement in July, they find that the new particle is looking more and more like a Higgs boson, the particle linked to the mechanism that gives mass to elementary particles. It remains an open question, however, whether this is the Higgs boson of the Standard Model of particle physics, or possibly the lightest of several bosons predicted in some theories that go beyond the Standard Model. Finding the answer to this question will take time.

Figure 1.19: CERN press release.

Chapter 2

The 2-Higgs Doublet Model

Disclaimer: A lot of material for this chapter has been taken from Refs. [10, 11, 12].

So far the experimental Higgs data are compatible with an SM Higgs boson. Still there is room for interpretations of the Higgs data within beyond the SM (BSM) Higgs physics. The SM contains only one complex Higgs doublet. A straightforward minimal extension is given by adding an additional singlet field or another Higgs doublet. When extending our model to BSM physics we have to be careful, however, not to violate experimental and theoretical constraints. Two major constraints are given by the ρ parameter and the severe limits on the existence of flavour-changing neutral currents (FCNC).

The ρ parameter constraint: The ρ parameter

$$\rho = \frac{M_W^2}{M_Z^2 \cos^2 \theta_W} \quad (2.1)$$

has been experimentally measured and is very close to one. In the SM the ρ parameter is determined by the Higgs structure of the theory and the tree-level value $\rho = 1$ is automatic. Introducing more generally n scalar multiplets ϕ_i with weak isospin I_i , weak hypercharge Y_i and VEV v_i of the neutral components, we have for the ρ parameter at tree level (demonstrate this)

$$\rho = \frac{\sum_{i=1}^n [I_i(I_i + 1) - \frac{1}{4}Y_i^2] v_i}{\sum_{i=1}^n \frac{1}{2}Y_i^2 v_i} . \quad (2.2)$$

Both $SU(2)$ singlets with $Y = 0$ and $SU(2)$ doublets with $Y = \pm 1$ satisfy

$$I(I + 1) = \frac{3}{4}Y^2 \quad (2.3)$$

and hence $\rho = 1$. Also models with larger $SU(2)$ multiplets, scalar particles with small or vanishing VEVs and models with triplets and a custodial $SU(2)$ global symmetry satisfy the ρ parameter constraint. But they lead to larger and more complex Higgs sectors.

Flavour-changing neutral currents: The existence of FCNC is experimentally severely constrained. In the SM tree-level FCNC are automatically absent, as the mass matrix automatically diagonalizes the Higgs-fermion couplings. This is in general not the case for non-minimal Higgs models. A solution to this problem is given by a theorem by Glashow

and Weinberg [13] and shall be discussed below.

Unitarity Constraints: Finally in any model of EWSB it must be ensured, that the amplitude for the scattering of longitudinal gauge bosons V ($V = W, Z$),

$$V_L V_L \rightarrow V_L V_L \quad (2.4)$$

or for fermions f scattering into longitudinal gauge bosons,

$$f_+ \bar{f}_+ \rightarrow V_L V_L, \quad (2.5)$$

where $+$ denotes the positive helicity of the fermion, do not violate unitarity bounds. This requires non-trivial cancellations of the Feynman diagrams contributing to a process. For example, in $WW \rightarrow WW$ scattering, the cancellation happens in the SM due to the existence of a light Higgs boson H with its couplings to the W bosons given by $g_{HWW} = gm_W$. In models with extended Higgs sectors it is not necessary that a single scalar boson ensures the unitary constraints. It is only necessary that sum rules for the scalar boson h_i couplings to VV and $f\bar{f}$ are fulfilled, namely

$$\sum_i g_{h_i VV}^2 = g_{HVV}^2 \quad (2.6)$$

and

$$\sum_i g_{h_i VV} g_{h_i f\bar{f}} = g_{HVV} g_{Hf\bar{f}}. \quad (2.7)$$

Note that these sum rules only hold for models with doublet and singlet Higgs fields. In extensions with triplets or higher Higgs representations there are more complicated sum rules.

The 2-Higgs Doublet Model (2HDM) with 2 complex Higgs doublets is - together with the singlet extension - the simplest possible extension of the SM and shall be discussed in the following. Besides the simple fact that extended Higgs sectors have not been ruled out yet experimentally, one main motivation for considering 2HDMs is supersymmetry (SUSY). Supersymmetry requires the introduction of two Higgs doublets due to the structure of the superpotential and also in order to have an anomaly-free theory. Another motivation is the fact that within the SM it is impossible to generate a sufficiently large baryon asymmetry of the universe. On the other hand, 2HDMs have more freedom due to their enlarged parameter space and also additional sources for explicit or spontaneous CP violation. The latter is one of the three Sakharov conditions to generate the baryon asymmetry.¹

2.1 The Higgs Potential

The 2HDM has a very rich vacuum structure due to the large number of parameters. Taking care of respecting the $SU(2)_L \times U(1)_Y$ gauge symmetry and requiring that the theory is renormalizable in $d = 4$ dimensions, there are altogether 14 operator products possible built of the two Higgs doublets Φ_1 and Φ_2 and that have operator dimension ≤ 4 . The most general scalar potential can have CP-conserving, CP-violating and charge-violating

¹The three conditions are baryon number violating processes, C and CP violation and departure from the thermal equilibrium.

minima. When writing up the potential care has to be taken in defining the various bases and in distinguishing between parameters which can be rotated away and those which have physical implications. If we assume, that CP is conserved and not spontaneously broken and if we impose a discrete symmetry (under which $\Phi_1 \rightarrow -\Phi_1$ and $\Phi_2 \rightarrow \Phi_2$)² that eliminate from the potential all quartic terms odd in either of the doublets, while allowing for all real quadratic coefficients, one of which softly breaks these symmetries, then the most general scalar potential for two doublets Φ_1 and Φ_2 with hypercharge +1 is given by [11]

$$V = m_{11}^2 \Phi_1^\dagger \Phi_1 + m_{22}^2 \Phi_2^\dagger \Phi_2 - m_{12}^2 (\Phi_1^\dagger \Phi_2 + \Phi_2^\dagger \Phi_1) + \frac{\lambda_1}{2} (\Phi_1^\dagger \Phi_1)^2 + \frac{\lambda_2}{2} (\Phi_2^\dagger \Phi_2)^2 + \lambda_3 \Phi_1^\dagger \Phi_1 \Phi_2^\dagger \Phi_2 + \lambda_4 \Phi_1^\dagger \Phi_2 \Phi_2^\dagger \Phi_1 + \frac{\lambda_5}{2} \left[(\Phi_1^\dagger \Phi_2)^2 + (\Phi_2^\dagger \Phi_1)^2 \right], \quad (2.8)$$

where all parameters are real.³ In the minimum of the Higgs potential the real components of the Higgs doublets take the VEVs

$$\langle \Phi_1 \rangle = \begin{pmatrix} 0 \\ \frac{v_1}{\sqrt{2}} \end{pmatrix} \quad \text{and} \quad \langle \Phi_2 \rangle = \begin{pmatrix} 0 \\ \frac{v_2}{\sqrt{2}} \end{pmatrix}. \quad (2.9)$$

The two complex Higgs doublets contain eight real fields⁴,

$$\Phi_a = \begin{pmatrix} \phi_a^+ \\ \frac{v_a + \rho_a + i\eta_a}{\sqrt{2}} \end{pmatrix}, \quad a = 1, 2. \quad (2.10)$$

Three out of them provide the longitudinal degrees of freedom for the massive W^\pm and Z bosons. After EWSB we are hence left with five Higgs fields. Assuming CP conservation, we have two neutral scalars, one neutral pseudoscalar and two charged Higgs bosons. Expansion about the minima leads to the mass term for the charged Higgs bosons, given by

$$\mathcal{L}_{\phi^\pm, \text{mass}} = -[m_{12}^2 - (\lambda_4 + \lambda_5) \frac{v_1 v_2}{2}] (\phi_1^-, \phi_2^-) \underbrace{\begin{pmatrix} \frac{v_2}{v_1} & -1 \\ -1 & \frac{v_1}{v_2} \end{pmatrix}}_{\mathcal{M}'_C} \begin{pmatrix} \phi_1^+ \\ \phi_2^+ \end{pmatrix}. \quad (2.11)$$

Here we have already exploited the minimum conditions

$$\left. \frac{\partial V}{\partial \Phi_i^\dagger} \right|_{\langle \Phi_i \rangle = v_i / \sqrt{2}} = 0, \quad i = 1, 2, \quad (2.12)$$

which imply

$$m_{11}^2 + \frac{\lambda_1 v_1^2}{2} + \frac{\lambda_3 v_2^2}{2} = m_{12}^2 \frac{v_2}{v_1} - (\lambda_4 + \lambda_5) \frac{v_2^2}{2}, \quad (2.13)$$

$$m_{22}^2 + \frac{\lambda_2 v_2^2}{2} + \frac{\lambda_3 v_1^2}{2} = m_{12}^2 \frac{v_1}{v_2} - (\lambda_4 + \lambda_5) \frac{v_1^2}{2}. \quad (2.14)$$

The mass matrix is diagonalized by the orthogonal transformation matrix

$$\mathcal{U}_C = \begin{pmatrix} \cos \beta & \sin \beta \\ -\sin \beta & \cos \beta \end{pmatrix}, \quad (2.15)$$

²We come back to this point when we discuss the constraints from FCNC couplings.

³Note, that in [10], the parameter m_{11}^2 is called m_1^2 , m_{22}^2 is m_2^2 and m_{12}^2 is named m_3^2 .

⁴The real fields ρ_a , η_a and the real fields building up the charged field $\phi_a^\pm = \chi_a \mp i\zeta_a$ ($a = 1, 2$).

where

$$\tan \beta = \frac{v_2}{v_1}. \quad (2.16)$$

The parameter $\tan \beta$ is a key parameter of the model. In order to reproduce the W and Z boson masses as in the SM we have

$$v_1^2 + v_2^2 = v^2, \quad (2.17)$$

with

$$v^2 = \frac{1}{\sqrt{2}G_F} \approx (246.22)^2 (\text{GeV})^2, \quad (2.18)$$

where $G_F = 1.1663787 \times 10^{-5} \text{ GeV}^{-2}$ denotes the Fermi constant. The mass matrix Eq. (2.11) has one zero eigenvalue, which corresponds to the charged Goldstone boson G^\pm . The mass squared of the charged Higgs boson reads

$$m_{H^\pm}^2 = \left(\frac{m_{12}^2}{v_1 v_2} - \frac{\lambda_4 + \lambda_5}{2} \right) (v_1^2 + v_2^2) = M^2 - \frac{1}{2}(\lambda_4 + \lambda_5)v^2, \quad (2.19)$$

where we have introduced

$$M^2 = \frac{m_{12}^2}{\sin \beta \cos \beta}. \quad (2.20)$$

Due to CP-invariance, as assumed here, the imaginary and the real parts of the neutral scalar fields decouple. The mass term for the pseudoscalars is given by the imaginary components of the neutral Higgs fields and, again by exploiting the minimum conditions, can be cast into the form

$$\mathcal{L}_{\eta, \text{mass}} = -\frac{1}{2} \frac{m_A^2}{v_1^2 + v_2^2} (\eta_1, \eta_2) \underbrace{\begin{pmatrix} v_2^2 & -v_1 v_2 \\ -v_1 v_2 & v_1^2 \end{pmatrix}}_{\mathcal{M}'_P} \begin{pmatrix} \eta_1 \\ \eta_2 \end{pmatrix}. \quad (2.21)$$

The mass matrix is diagonalized by the orthogonal transformation matrix \mathcal{U}_P , for which at tree-level

$$\mathcal{U}_P = \mathcal{U}_C. \quad (2.22)$$

This leads to one neutral Goldstone boson G^0 and a pseudoscalar, denoted by A , with mass squared

$$m_A^2 = \left(\frac{m_{12}^2}{v_1 v_2} - \lambda_5 \right) (v_1^2 + v_2^2) = M^2 - \lambda_5 v^2. \quad (2.23)$$

Note, that when $m_{12} = 0$ and $\lambda_5 = 0$, then the pseudoscalar is massless. The reason behind this is the existence of an additional global $U(1)$ symmetry in that limit, which is spontaneously broken. The mass terms for the scalars, derived by collecting the bilinear terms of the real parts of the neutral Higgs fields and exploiting the minimum conditions, read

$$\mathcal{L}_{\rho, \text{mass}} = -\frac{1}{2} (\rho_1, \rho_2) \underbrace{\begin{pmatrix} m_{12}^2 \frac{v_2}{v_1} + \lambda_1 v_1^2 & -m_{12}^2 + \lambda_{345} v_1 v_2 \\ -m_{12}^2 + \lambda_{345} v_1 v_2 & m_{12}^2 \frac{v_1}{v_2} + \lambda_2 v_2^2 \end{pmatrix}}_{\mathcal{M}_N} \begin{pmatrix} \rho_1 \\ \rho_2 \end{pmatrix}, \quad (2.24)$$

where we have defined

$$\lambda_{345} \equiv \lambda_3 + \lambda_4 + \lambda_5 . \quad (2.25)$$

The mass matrix is diagonalized by the orthogonal transformation matrix

$$\mathcal{U}_N = \begin{pmatrix} \cos \alpha & \sin \alpha \\ -\sin \alpha & \cos \alpha \end{pmatrix} . \quad (2.26)$$

The mixing angle α is given in terms of the matrix elements of the mass matrix \mathcal{M}_N as

$$\sin 2\alpha = \frac{2\mathcal{M}_{12}}{\sqrt{(\mathcal{M}_{11} - \mathcal{M}_{22})^2 + 4\mathcal{M}_{12}^2}} \quad (2.27)$$

$$\cos 2\alpha = \frac{\mathcal{M}_{11} - \mathcal{M}_{22}}{\sqrt{(\mathcal{M}_{11} - \mathcal{M}_{22})^2 + 4\mathcal{M}_{12}^2}} \quad (2.28)$$

and

$$\tan 2\alpha = \frac{(M^2 - \lambda_{345}v^2) \sin 2\beta}{(M^2 - \lambda_1v^2) \cos^2 \beta - (M^2 - \lambda_2v^2) \sin^2 \beta} . \quad (2.29)$$

This leads to the CP-even mass eigenstates h and H

$$H = \rho_1 \cos \alpha + \rho_2 \sin \alpha \quad (2.30)$$

$$h = -\rho_1 \sin \alpha + \rho_2 \cos \alpha , \quad (2.31)$$

with the mass values

$$m_{H,h}^2 = \frac{1}{2} \left[\mathcal{M}_{11} + \mathcal{M}_{22} \pm \sqrt{(\mathcal{M}_{11} - \mathcal{M}_{22})^2 + 4\mathcal{M}_{12}^2} \right] . \quad (2.32)$$

By convention the lighter CP-even state is called h and the heavier one H . Note that the SM Higgs boson would be

$$\begin{aligned} H^{\text{SM}} &= \rho_1 \cos \beta + \rho_2 \sin \beta \\ &= H \cos(\alpha - \beta) - h \sin(\alpha - \beta) . \end{aligned} \quad (2.33)$$

The SM Higgs boson hence corresponds to h for $\cos \alpha = \sin \beta$ and $\sin \alpha = -\cos \beta$. It corresponds to H for $\cos \alpha = \cos \beta$ and $\sin \alpha = \sin \beta$. That Eq. (2.33) defines the SM Higgs can be seen by multiplying the Higgs doublets with the mixing matrix \mathcal{U}_C , respectively \mathcal{U}_P ,

$$\begin{pmatrix} \cos \beta & \sin \beta \\ -\sin \beta & \cos \beta \end{pmatrix} \begin{pmatrix} \Phi_1 \\ \Phi_2 \end{pmatrix} = \begin{pmatrix} \cos \beta \Phi_1 + \sin \beta \Phi_2 \\ -\sin \beta \Phi_1 + \cos \beta \Phi_2 \end{pmatrix} , \quad (2.34)$$

This leads to two Higgs doublets, one of which

$$\begin{aligned} \Phi_1^{\text{HB}} &= \cos \beta \Phi_1 + \sin \beta \Phi_2 = \begin{pmatrix} \cos \beta \phi_1^+ + \sin \beta \phi_2^+ \\ \frac{1}{\sqrt{2}} [\cos \beta (v_1 + \rho_1 + i\eta_1) + \sin \beta (v_2 + \rho_2 + i\eta_2)] \end{pmatrix} \\ &= \begin{pmatrix} G^\pm \\ \frac{1}{\sqrt{2}} [iG^0 + (\cos \beta \rho_1 + \sin \beta \rho_2) + v] \end{pmatrix} \equiv \begin{pmatrix} G^\pm \\ \frac{1}{\sqrt{2}} [iG^0 + S_1 + v] \end{pmatrix} , \end{aligned} \quad (2.35)$$

contains the massless Goldstone bosons and the VEV v in the neutral component, so that $S_1 \equiv (\cos \beta \rho_1 + \sin \beta \rho_2)$ can be identified with the SM Higgs boson. The superscript HB stands for 'Higgs Basis'. The other Higgs doublet reads

$$\begin{aligned} \Phi_2^{\text{HB}} &= -\sin \beta \Phi_1 + \cos \beta \Phi_2 = \begin{pmatrix} -\sin \beta \phi_1^+ + \cos \beta \phi_2^+ \\ \frac{1}{\sqrt{2}} [-\sin \beta (v_1 + \rho_1 + i\eta_1) + \cos \beta (v_2 + \rho_2 + i\eta_2)] \end{pmatrix} \\ &= \begin{pmatrix} H^+ \\ \frac{1}{\sqrt{2}} (-\sin \beta \rho_1 + \cos \beta \rho_2) + \frac{i}{\sqrt{2}} (-\sin \beta \eta_1 + \cos \beta \eta_2) \end{pmatrix} \equiv \begin{pmatrix} H^+ \\ \frac{S_2 + iS_3}{\sqrt{2}} \end{pmatrix}. \end{aligned} \quad (2.36)$$

The advantage of the Higgs Basis is that the three Goldstone fields G^\pm and G^0 get isolated as components of Φ_1 . The three neutral scalar mass eigenstates of the physical scalar spectrum, $\varphi_i^0 = (h, H, A)^T$ are related through an orthogonal transformation \mathcal{R} with the S_i fields,

$$\varphi_i^0 = \mathcal{R}_{ij} S_j. \quad (2.37)$$

In general the CP-odd component S_3 mixes with the CP-even fields $S_{1,2}$ and the resulting mass eigenstates do not have a definite CP quantum number. If the scalar potential is CP symmetric this admixture disappears. In this case $A \equiv S_3$.

Without loss of generality it can be assumed that β is in the first quadrant, *i.e.* that both v_1 and v_2 are non-negative and real. Furthermore, π can be added to α , which inverts the sign of both the h and H fields, without affecting any physics. The angle α will be chosen either in the first or the fourth quadrant.

The decoupling and the non-decoupling effect:

The masses of the heavier Higgs bosons (H, H^\pm and A) take the form

$$m_\Phi^2 = M^2 + \lambda_i v^2 (+\mathcal{O}(v^4/M^2)), \quad (2.38)$$

where $\Phi \equiv H, H^\pm, A$ and λ_i is a linear combination of λ_1 – λ_5 . In case $M^2 \gg \lambda_i v^2$ the mass m_Φ^2 is determined by the soft-breaking scale of the discrete symmetry, M^2 . The effective theory below M is then described by one Higgs doublet. And all the tree-level couplings related to the lightest Higgs boson h approach SM values. The loop effects of Φ vanish in the large mass limit due to the decoupling theorem.

In case M^2 is limited to be at the weak scale ($M^2 \lesssim \lambda_i v^2$) a large value of m_ϕ is realized by taking λ_i to be large, so that one is in the strong coupling regime. The squared mass of Φ is then effectively proportional to λ_i , so that the decoupling theorem does not apply, leading to a power-like contribution of m_ϕ in the radiative corrections. This effect is called the non-decoupling effect of Φ . However, theoretical and experimental constraints have to be considered. Thus too large λ_i lead to the breakdown of the validity of perturbation theory. And low-energy precision data impose important constraints on the model parameters.

Parameters of the Higgs Potential:

The parameters of the Higgs potential are $m_{11}^2, m_{22}^2, m_{12}^2$ and λ_1 – λ_5 . They can be expressed in terms of eight 'physical' parameters, which are the four Higgs mass parameters m_h, m_H, m_A, m_{H^\pm} , the two mixing angles α, β , the vacuum expectation value v and the soft-breaking scale of the discrete symmetry, M . The quartic coupling constants can be expressed in terms of these parameters. (Derive the expressions!)

2.2 The problem with flavour conservation

The 2HDM faces the serious problem of possible FCNCs at tree-level. To see this let us look at *e.g.* the Yukawa Lagrangian. The most general Yukawa Lagrangian is given by

$$\begin{aligned} \mathcal{L}_Y = & -\left\{ \bar{Q}'_L(\Gamma_1\Phi_1 + \Gamma_2\Phi_2)D'_R - \bar{Q}'_L(\Delta_1\tilde{\Phi}_1 + \Delta_2\tilde{\Phi}_2)U'_R \right. \\ & \left. + \bar{L}'(\Pi_1\Phi_1 + \Pi_2\Phi_2)E'_R + h.c. \right\}, \end{aligned} \quad (2.39)$$

where Q'_L, L'_L denote the left-handed quark and lepton doublets and $Q \equiv (U, D)^T$, $L \equiv (\nu, E)^T$, with $U \equiv (u, c, t)^T$, $D \equiv (d, s, b)^T$, $\nu \equiv (\nu_e, \nu_\mu, \nu_\tau)^T$ and $E \equiv (e, \mu, \tau)^T$. The indices L, R denote left- and right-handed fermions f given by

$$f_{L,R} = P_{L,R}f \equiv \frac{1}{2}(1 \mp \gamma_5)f. \quad (2.40)$$

We have defined $\tilde{\Phi}_a = (\Phi_a^T \epsilon)^\dagger$, with

$$\epsilon = \begin{pmatrix} 0 & 1 \\ -1 & 0 \end{pmatrix}. \quad (2.41)$$

The couplings Γ_a, Δ_a and Π_a ($a = 1, 2$) are 3×3 complex matrices in flavour space. In the Higgs basis the Lagrangian can be cast into the form

$$\begin{aligned} \mathcal{L}_Y = & -\frac{\sqrt{2}}{v} \left\{ \bar{Q}'_L(M'_d\Phi_1^{\text{HB}} + Y'_d\Phi_2^{\text{HB}})D'_R - \bar{Q}'_L(M'_u\tilde{\Phi}_1^{\text{HB}} + Y'_u\tilde{\Phi}_2^{\text{HB}})U'_R \right. \\ & \left. + \bar{L}'(M'_l\Phi_1^{\text{HB}} + Y'_l\Phi_2^{\text{HB}})E'_R + h.c. \right\}, \end{aligned} \quad (2.42)$$

where M'_f ($f = d, u, l$) are the non-diagonal fermion mass matrices. The matrices Y'_f contain the Yukawa couplings to the scalar doublet with zero vacuum expectation value.

In the basis of the mass eigenstates D, U, E, ν , with diagonal mass matrices M_f ($M_\nu = 0$), the corresponding matrices Y_f are in general non-diagonal and unrelated to the fermion masses. Therefore the Yukawa Lagrangian leads to FCNC couplings, as there are two different Yukawa matrices coupling to a right-handed fermion field. These can in general not be diagonalized simultaneously. Thus neutral Higgs scalars ϕ can mediate FCNC, as *e.g.* $\bar{d}s\phi$. This would lead to serious phenomenological conflicts. This coupling would lead *e.g.* to $K-\bar{K}$ mixing at tree level. Assuming the coupling to be as large as the b -quark Yukawa coupling, this would require the mass of the exchanged scalar to exceed 10 TeV, in order to achieve a suppression that is in accordance with the experiments.

The problem can be avoided by forcing one of the two matrices to be zero, which can be achieved by imposing that only one scalar doublet couples to a given right-handed fermion field. In other words, if all fermions with the same quantum numbers (so that they can mix) couple to the same Higgs multiplet, then FCNCs are absent. This has been stated in the Paschos-Glashow-Weinberg theorem [14]. It says that a necessary and sufficient condition for the absence of FCNCs at tree level is that all fermions of a given charge and helicity transform according to the same irreducible representation of $SU(2)$, correspond to the same eigenvalue of T_3 and that a basis exists in which they receive their contributions to the mass matrix from a single source. For the SM with left-handed doublets and right-handed singlets, this means that all right-handed quarks of a given charge must couple to a single Higgs multiplet. In the 2HDM, this can only be ensured by introducing discrete or continuous symmetries.

In the 2HDM there are two possibilities to achieve this:

- type I 2HDM: All quarks couple to just one of the Higgs doublets (conventionally chosen to be Φ_2).
- type II 2HDM: The $Q = 2/3$ right-handed (RH) quarks couple to one Higgs doublet (conventionally chosen to be Φ_2) and the $Q = -1/3$ RH quarks couple to the other (Φ_1).

In order to get the type I 2HDM a simple discrete symmetry $\Phi_1 \rightarrow -\Phi_1$ is imposed. For the type II 2HDM a $\Phi_1 \rightarrow -\Phi_1$, $d_R^i \rightarrow -d_R^i$ discrete symmetry is enforced. Note, that SUSY models lead to the same Yukawa couplings as the type II model. They use, however, continuous symmetries.

In the type I and type II 2HDMs it is conventionally assumed, that the right-handed leptons satisfy the same discrete symmetry as the d_R^i , so that the leptons couple to the same Higgs boson as the down-type quarks. The Glashow-Weinberg theorem, however, does not require this. There are therefore two more possibilities:

- Lepton-specific model: The RH quarks all couple to Φ_2 and the RH leptons couple to Φ_1 .
- Flipped model: The RH up-type quarks couple to Φ_2 , the RH down-type quarks couple to Φ_1 , as in type II, but now the RH leptons couple to Φ_2 .

There circulate a lot of different names for these models in the literature. Thus Model III and Model IV were used for the flipped and lepton-specific models, respectively, in one of the earliest works on them. In other papers lepton-specific and flipped were named, respectively, Model I and Model II. Also the terms IIA and IIB were used. Recently, lepton-specific was called X-type and flipped Y-type models.

The explicit implementation of the discrete symmetry is scalar-basis dependent. If it is imposed in the Higgs Basis, all fermions are forced to couple to the field Φ_1^{HB} in order to get non-vanishing masses. This *inert* doublet model provides a natural frame for dark matter. Note, however, that although Φ_2^{HB} does not couple to fermions, it has nevertheless electroweak interactions.

Tree-level FCNC interactions can be avoided in a softer and more general way by requiring the alignment in flavour space of the Yukawa couplings of the two scalar doublets. A convenient way to implement this condition is given by the form

$$\Gamma_2 = \xi_d e^{-i\theta} \Gamma_1, \quad \Delta_2 = \xi_u^* e^{i\theta} \Delta_1, \quad \Pi_2 = \xi_l e^{-i\theta} \Pi_1. \quad (2.43)$$

The proportionality parameters ξ_f are arbitrary complex numbers. The explicit phases $e^{\mp i\theta}$ can be introduced to cancel the relative global phases between the two scalar doublets. They will be omitted in the following. Through the Yukawa alignment the Y_f' and M_f' matrices are guaranteed to be proportional to each other, so that they can be diagonalized simultaneously, leading to

$$Y_{d,l} = \zeta_{d,l} M_{d,l}, \quad Y_u = \zeta_u^* M_u, \quad \zeta_f \equiv \frac{\xi_f - \tan \beta}{1 + \xi_f \tan \beta}. \quad (2.44)$$

The Yukawa interactions in terms of the mass eigenstate fields then take the form

$$\begin{aligned} \mathcal{L}_Y = & -\frac{\sqrt{2}}{v}H^+\bar{U}[\zeta_dVM_dP_R - \zeta_uM_uVP_L]D - \frac{\sqrt{2}}{v}H^+\zeta_l\bar{\nu}M_lP_RE \\ & -\frac{1}{v}\sum_{\varphi_i^0,f} \varphi_i^0 y_f^{\varphi_i^0} \bar{f}M_fP_Rf + h.c. , \end{aligned} \quad (2.45)$$

where V is the Cabibbo-Kobayashi-Maskawa (CKM) matrix. The flavour alignment of the Yukawa couplings leads to a very specific structure of the scalar couplings to the fermions:

- i) All fermion couplings of the physical scalar fields are proportional to the corresponding fermion mass matrices.
- ii) The neutral Yukawa couplings are diagonal in flavour space. The couplings of the physical scalar fields h, H and A are proportional to the corresponding elements of the orthogonal matrix \mathcal{R} , namely

$$y_{d,l}^{\varphi_i^0} = \mathcal{R}_{i1} + (\mathcal{R}_{i2} + i\mathcal{R}_{i3})\zeta_{d,l} \quad (2.46)$$

$$y_u^{\varphi_i^0} = \mathcal{R}_{i1} + (\mathcal{R}_{i2} - i\mathcal{R}_{i3})\zeta_u^* . \quad (2.47)$$

- iii) The only source of flavour-changing couplings is given by the CKM matrix V . It regulates the quark couplings of the W^\pm bosons and the charged scalars H^\pm .
- iv) All leptonic couplings are diagonal in flavour space. This is because we assume the neutrinos to be massless in our low-energy Lagrangian. (Although we know in the meantime that the neutrinos have mass.) Since we assume the neutrinos to be massless the leptonic mixing matrix can be reabsorbed through a redefinition of the neutrino fields.
- v) The only new couplings introduced by the Yukawa Lagrangian are the three parameters ζ_f , which encode all possible freedom allowed by the alignment conditions. The couplings satisfy universality among the different generations, as all fermions of a given electric charge have the same universal coupling ζ_f . Furthermore, the parameters ζ_f are invariant under global $SU(2)$ transformations of the scalar fields [16], *i.e.* $\Phi_a \rightarrow \Phi'_a = U_{ab}\Phi_b$. This means that they are independent of the basis choice adopted in the scalar space.
- vi) The models where a single scalar doublet couples to each type of right-handed fermions are recovered by taking the appropriate limits $\xi_f \rightarrow 0$ or $\xi_f \rightarrow \infty$, *i.e.* $\zeta_f \rightarrow -\tan\beta$ or $\zeta_f \rightarrow \cot\beta$. Thus the type-I model corresponds to $(\xi_d, \xi_u, \xi_l) = (\infty, \infty, \infty)$, type II to $(0, \infty, 0)$, the lepton-specific to $(\infty, \infty, 0)$ and the flipped model to $(0, \infty, \infty)$. (Compare with Table 2.1.) The *inert* model corresponds to $\zeta_f = 0$ ($\xi_f = \tan\beta$).
- vii) The ζ_f can be arbitrary complex numbers, so that one can have new sources of CP violation without tree-level FCNCs.

We will now determine the Yukawa couplings. In the type II model, *e.g.* the Yukawa Lagrangian is given by⁵

$$\begin{aligned} \mathcal{L}_Y = & - \left\{ \bar{E}_R \begin{pmatrix} h_e & 0 & 0 \\ 0 & h_\mu & 0 \\ 0 & 0 & h_\tau \end{pmatrix} \Phi_1^\dagger E_L + \bar{D}'_R V \begin{pmatrix} h_d & 0 & 0 \\ 0 & h_s & 0 \\ 0 & 0 & h_b \end{pmatrix} V^\dagger \Phi_1^\dagger \begin{pmatrix} U \\ D' \end{pmatrix}_L \right. \\ & \left. - \bar{U}_R \begin{pmatrix} h_u & 0 & 0 \\ 0 & h_c & 0 \\ 0 & 0 & h_t \end{pmatrix} \Phi_2^T \epsilon \begin{pmatrix} U \\ D' \end{pmatrix}_L + h.c. \right\}. \end{aligned} \quad (2.48)$$

Here $U \equiv (u, c, t)^T$, $D \equiv (d, s, b)^T$ and $E \equiv (e, \mu, \tau)^T$. The h_f denote the various Yukawa couplings. Coupling the Higgs doublets for the various models as described above and rotating to the mass eigenstates, one gets, in the notation of Ref. [15], the Yukawa Lagrangian

$$\begin{aligned} \mathcal{L}_{\text{Yukawa}}^{\text{2HDM}} = & - \sum_{f=u,d,l} \frac{m_f}{v} \left(\xi_h^f \bar{f} f h + \xi_H^f \bar{f} f H - i \xi_A^f \bar{f} \gamma_5 f A \right) \\ & - \left\{ \frac{\sqrt{2} V_{ud}}{v} \bar{u} (m_u \xi_A^u P_L + m_d \xi_A^d P_R) d H^+ + \frac{\sqrt{2} m_l \xi_A^l}{v} \bar{\nu}_L l_R H^+ + h.c. \right\} \end{aligned} \quad (2.49)$$

Here we have replaced the Yukawa coupling h_f of the fermions f to the Higgs boson by $\sqrt{2} m_f / v_i$. In the Lagrangian the u, d, l, ν stand for all three generations. The Lagrangian defines the parameters $\xi_h^f, \xi_H^f, \xi_A^f$. They are defined in Table 2.1.

	Type I	Type II	Lepton-specific	Flipped
ξ_h^u	$\cos \alpha / \sin \beta$	$\cos \alpha / \sin \beta$	$\cos \alpha / \sin \beta$	$\cos \alpha / \sin \beta$
ξ_h^d	$\cos \alpha / \sin \beta$	$-\sin \alpha / \cos \beta$	$\cos \alpha / \sin \beta$	$-\sin \alpha / \cos \beta$
ξ_h^l	$\cos \alpha / \sin \beta$	$-\sin \alpha / \cos \beta$	$-\sin \alpha / \cos \beta$	$\cos \alpha / \sin \beta$
ξ_H^u	$\sin \alpha / \sin \beta$	$\sin \alpha / \sin \beta$	$\sin \alpha / \sin \beta$	$\sin \alpha / \sin \beta$
ξ_H^d	$\sin \alpha / \sin \beta$	$\cos \alpha / \cos \beta$	$\sin \alpha / \sin \beta$	$\cos \alpha / \cos \beta$
ξ_H^l	$\sin \alpha / \sin \beta$	$\cos \alpha / \cos \beta$	$\cos \alpha / \cos \beta$	$\sin \alpha / \sin \beta$
ξ_A^u	$\cot \beta$	$\cot \beta$	$\cot \beta$	$\cot \beta$
ξ_A^d	$-\cot \beta$	$\tan \beta$	$-\cot \beta$	$\tan \beta$
ξ_A^l	$-\cot \beta$	$\tan \beta$	$\tan \beta$	$-\cot \beta$

Table 2.1: The u, d, l (they stand for all three generations) Yukawas couplings to the neutral Higgs bosons h, H, A in the four different models.

2.3 Branching Ratios

For the determination of the Higgs decays widths, we also need the couplings to the gauge bosons. The couplings of the Higgs bosons to the gauge bosons are derived from

$$\sum_{i=1}^2 (D_\mu \Phi_i)^\dagger (D^\mu \Phi_i), \quad (2.50)$$

⁵Compare with ‘‘Theoretische Teilchenphysik’’ winter semester 2013/14, section 2.7.2.

with

$$D_\mu = \partial_\mu + i\frac{g}{2}\vec{\tau}\vec{W}_\mu + i\frac{g'}{2}B_\mu, \quad (2.51)$$

where $\vec{\tau} = (\tau_1, \tau_2, \tau_3)^T$ in terms of the Pauli matrices. Using $\Phi_i = (\phi_i^+, 1/\sqrt{2}(v_i + \rho_i + i\eta_i))^T$ and

$$\rho_1 = Hc_\alpha - hs_\alpha, \quad \rho_2 = Hs_\alpha + hc_\alpha, \quad (2.52)$$

$$\eta_1 = G^0c_\beta - As_\beta, \quad \eta_2 = G^0s_\beta + Ac_\beta, \quad (2.53)$$

one finds for all four 2HDM models for the Higgs couplings to the gauge bosons normalized to the corresponding SM coupling $g_{H^{\text{SM}}VV}$ ($V = W, Z$)

$$g_{hWW} = \sin(\beta - \alpha)g_{H^{\text{SM}}WW}, \quad g_{hZZ} = \sin(\beta - \alpha)g_{H^{\text{SM}}ZZ}, \quad (2.54)$$

$$g_{HWW} = \cos(\beta - \alpha)g_{H^{\text{SM}}WW}, \quad g_{HZZ} = \cos(\beta - \alpha)g_{H^{\text{SM}}ZZ}, \quad (2.55)$$

$$g_{A WW} = g_{A ZZ} = 0. \quad (2.56)$$

Note that in the 2HDM the Higgs couplings to the gauge bosons are always suppressed compared to the SM, and in the case of the pseudoscalar they vanish.

In the 2HDM we can have additional decays of the neutral Higgs bosons, such as Higgs-to-Higgs decays

$$h, H \rightarrow AA, \quad H \rightarrow hh, \quad h, H \rightarrow H^+H^-, \quad (2.57)$$

and Higgs decays into a Higgs boson and a gauge boson,

$$h, H \rightarrow ZA, \quad h, H, A \rightarrow W^\pm H^\mp, \quad A \rightarrow Zh, ZH. \quad (2.58)$$

The Higgs-to-Higgs decays require the derivation of the trilinear Higgs self-couplings (exercise!). They can be expressed in terms of the Higgs masses, M , α and β and can be found in Ref. [10] in Eqs. (E1)-(E6), (E11) and (E12). The Eqs. (E9), (E10), (E15) and (E16) contain the Higgs-Higgs-gauge boson couplings.

With these couplings at hand the decay widths and branching ratios can be calculated. There are several public programs that have implemented the calculation of the branching ratios of the 2HDM including the state-of-the-art higher order corrections, such as:

- HDECAY

Ref.: A. Djouadi, J. Kalinowski and M. Spira, *Comput. Phys. Commun.* **108** (1998) 56 [hep-ph/9704448]; A. Djouadi, M. M. Mühlleitner and M. Spira, arXiv:1801.09506 [hep-ph].

webpage: <http://tiger.web.psi.ch/hdecay/>

- 2HDMC

Ref.: D. Eriksson, J. Rathsman and O. Stål, *Comput. Phys. Commun.* **181** (2010) 189 [arXiv:0902.0851 [hep-ph]]; D. Eriksson, J. Rathsman and O. Stål, *Comput. Phys. Commun.* **181** (2010) 833.

webpage: <http://2hdmc.hepforge.org/>

Exercise: Determine the branching ratios. Produce plots for the branching ratios of respectively, H, A, H^\pm as a function of their mass. Choose $m_h = 125$ GeV, $\sin(\beta - \alpha) = 0.9$ (to be close to the SM) and two values of $\tan\beta$, $\tan\beta = 2, 10$. For the time being, we are not interested in Higgs-to-Higgs decays, so that m_{12}^2 can be chosen arbitrarily. For simplicity choose H and H^\pm to be close in mass (*e.g.* 150 and 600 GeV, respectively). As for the h mass, choose it such that in one case the $H \rightarrow H^+H^-$ and $H \rightarrow ZA$ decays are possible, in the other case not.

2.4 Higgs Production

For the neutral Higgs bosons of the 2HDM the same production mechanisms apply as in the SM. The dominant production process at the LHC is given by gluon fusion. The cross section can readily be taken over from the SM by making the appropriate replacements of the Higgs couplings to the top and bottom quarks. So we have for $\phi = h, H, A$

$$\sigma(gg \rightarrow \phi) = m_\phi^2 \delta(\hat{s} - m_\phi^2) \hat{\sigma}, \quad (2.59)$$

where \hat{s} denotes the partonic c.m. energy and

$$\hat{\sigma} = \frac{G_F \alpha_s^2}{512 \sqrt{2} \pi} \left| \sum_{q=t,b} g_{\phi qq} A_{1/2}^\phi(\tau_q) \right|^2. \quad (2.60)$$

Here we have defined $\tau_q = 4m_q^2/m_\phi^2$ and the Yukawa coupling modification factors for the four 2HDM models are summarised in Tab. 2.1. Furthermore, we have the form factors

$$A_{1/2}^{h/H} = 2\tau[1 + (1 - \tau)f(\tau)] \quad (2.61)$$

$$A_{1/2}^A = 2\tau f(\tau), \quad (2.62)$$

with $f(\tau)$ defined in Eq. (1.24). For large quark masses, *i.e.* $\tau_q \ll 1$, they approach

$$A_{1/2}^{h/H} \rightarrow \frac{4}{3} \quad \text{and} \quad A_{1/2}^A \rightarrow 2. \quad (2.63)$$

Note in particular, that while b -quark loops in the SM do not play a role in the type II and the flipped 2HDMs they can become crucial for large values of $\tan\beta$ as the Higgs couplings to down-type quarks are proportional to $\tan\beta$.

The production cross sections for h and H in gauge boson fusion and Higgs radiation can be obtained from the corresponding SM cross sections by multiplying them with the coupling modification factors $\sin^2(\beta - \alpha)$ for h and $\cos^2(\beta - \alpha)$ for H . The pseudoscalar does not couple to the gauge bosons and cannot be produced through these processes. The $t\bar{t}\phi$ production cross section is obtained from the SM formula by multiplying it with $(\cos\alpha/\sin\beta)^2$ for h , $(\sin\alpha/\sin\beta)^2$ for H and $\cot^2\beta$ for A in all four 2HDM models. In the type II and flipped 2HDMs also $b\bar{b}\phi$ production can become important due to the $\tan\beta$ enhanced Higgs couplings to b -quarks for large values of $\tan\beta$.

In the 2HDM there are further production mechanisms. Thus a resonantly produced heavy scalar can decay into a Higgs pair. Higgs bosons can also be produced in di-Higgs production through non-resonant channels and from gauge bosons produced in the Drell-Yan process, that subsequently decay into a Higgs pair. As the 2HDM has a large parameter

space and the trilinear couplings are not given by the gauge couplings (as in supersymmetric theories) the double Higgs production cross sections can in general be larger than in the Minimal Supersymmetric extension of the SM (MSSM). Charged Higgs bosons finally can be produced in H^+H^- production or, if they are light enough, from top decays.

2.5 Type II 2HDM and the MSSM

As stated earlier the Higgs coupling structure to the fermions of the type II 2HDM is the same as in the MSSM. However, there are some crucial differences between these models:

- The type II 2HDM does not have a strict upper bound on the mass of the lightest Higgs boson. This is the case in the MSSM, as the Higgs potential, due to supersymmetry, is given in terms of the gauge couplings.
- For the same reason in the 2HDM the scalar self-couplings are now arbitrary.
- Also the mixing angle α , which in the MSSM is given in terms of $\tan\beta$ and the scalar and pseudoscalar masses, is now arbitrary.
- In the MSSM the charged scalar and pseudoscalar masses are so close that the decay of the charged Higgs boson into a pseudoscalar and a real W is kinematically forbidden, while it is generally allowed in the type II 2HDM.

2.6 The Scalar Sector of the 2HDM

In its most general form the Higgs potential has 14 independent parameters. The Higgs doublets Φ_1 and Φ_2 are not physical observables, only the scalar mass eigenstates are physical particles. One therefore has the freedom to redefine the doublets, provided the form of their kinetic terms is preserved. Through such basis changes some of the parameters in the potential can be absorbed. They are essential to understand the number of physical parameters really present in the potential.

It is common to impose a variety of global symmetries on the 2HDM, *e.g.* in order to avoid tree-level FCNC couplings. Thereby the number of free parameters is reduced. It has been proven that there are only *six* such symmetries which have distinct effects on the scalar potential. The resulting six models have different physical implications:

different spectra of scalars, different interactions with gauge bosons, in some cases predictions of massless axions or potential dark matter candidates.

The scalar potential determines the vacuum of the 2HDM. Contrary to the SM this vacuum is not unique. With two Higgs doublets it is possible that the model spontaneously breaks the CP symmetry. For certain parameter values of the potential it is also possible to have vacua that violate the electromagnetic symmetry and thus give mass to the photon. These have to be avoided of course. Even if only vacua are considered that preserve both CP and the usual gauge symmetries of the SM, the 2HDM has a rich vacuum structure. Thus some potentials can have two different electromagnetism-preserving minima, with different predictions for the masses of the gauge bosons for example. The 2HDM, however, has a feature which distinguishes it from other multi-Higgs models, such as SUSY or the 3HDM:

Its vacua are stable and no tunneling from a neutral, CP-conserving vacuum to a deeper, CP- or charge-breaking vacuum is possible. Vice-versa, any CP- or charge-breaking minimum that one finds is guaranteed to be the global minimum of the model.

Not all values of the parameters of the 2HDM potential, however, ensure a stable minimum, unless the potential can be ensured to be bounded from below. This basic requirement imposes constraints on the quartic scalar couplings and translates in possibly severe bounds on the masses of the physical scalar particles through renormalization-group improvement.

2.6.1 Notations of the Scalar Potential

Notation 1: The most general renormalizable scalar potential can be written as [17]

$$\begin{aligned}
V_H = & m_{11}^2 \Phi_1^\dagger \Phi_1 + m_{22}^2 \Phi_2^\dagger \Phi_2 - m_{12}^2 \left(\Phi_1^\dagger \Phi_2 + \Phi_2^\dagger \Phi_1 \right) + \frac{\lambda_1}{2} \left(\Phi_1^\dagger \Phi_1 \right)^2 + \frac{\lambda_2}{2} \left(\Phi_2^\dagger \Phi_2 \right)^2 \\
& + \lambda_3 (\Phi_1^\dagger \Phi_1) (\Phi_2^\dagger \Phi_2) + \lambda_4 (\Phi_1^\dagger \Phi_2) (\Phi_2^\dagger \Phi_1) \\
& + \left[\frac{\lambda_5}{2} (\Phi_1^\dagger \Phi_2)^2 + \lambda_6 (\Phi_1^\dagger \Phi_1) (\Phi_1^\dagger \Phi_2) + \lambda_7 (\Phi_2^\dagger \Phi_2) (\Phi_1^\dagger \Phi_2) + h.c. \right]. \quad (2.64)
\end{aligned}$$

The parameters m_{11}^2 , m_{22}^2 and $\lambda_{1,2,3,4}$ are real, whereas m_{12}^2 and $\lambda_{5,6,7}$ are complex. This leads to 14 parameters for the Higgs potential of Eq. (2.64). However, the freedom to redefine the basis means that in reality only eleven degrees of freedom are physical.

Notation 2: An alternative notation has been given in [18] and reads

$$V_H = \sum_{a,b=1}^2 \mu_{ab} \Phi_a^\dagger \Phi_b + \frac{1}{2} \sum_{a,b,c,d=1}^2 \lambda_{ab,cd} (\Phi_a^\dagger \Phi_b) (\Phi_c^\dagger \Phi_d), \quad (2.65)$$

where by definition

$$\lambda_{ab,cd} = \lambda_{cd,ab}. \quad (2.66)$$

Hermiticity in Eq. (2.65) implies

$$\mu_{ab} = \mu_{ba}^* \quad \text{and} \quad \lambda_{ab,cd} = \lambda_{ba,dc}^*. \quad (2.67)$$

The notation of Eq. (2.65) is useful for the study of invariants, basis transformations and symmetries. The correspondance between notation 1 and 2 is given by

$$\begin{aligned}
\mu_{11} &= m_{11}^2, & \mu_{22} &= m_{22}^2, \\
\mu_{12} &= -m_{12}^2, & \mu_{21} &= -m_{12}^{2*}, \\
\lambda_{11,11} &= \lambda_1, & \lambda_{22,22} &= \lambda_2, \\
\lambda_{11,22} = \lambda_{22,11} &= \lambda_3, & \lambda_{12,21} &= \lambda_{21,12} = \lambda_4, \\
\lambda_{12,12} &= \lambda_5, & \lambda_{21,21} &= \lambda_5^*, \\
\lambda_{11,12} = \lambda_{12,11} &= \lambda_6, & \lambda_{11,21} &= \lambda_{21,11} = \lambda_6^*, \\
\lambda_{22,12} = \lambda_{12,22} &= \lambda_7, & \lambda_{22,21} &= \lambda_{21,22} = \lambda_7^*.
\end{aligned}$$

Notation 3: While the previous notations consider the scalar doublets Φ_a ($a = 1, 2$) individually, the third notation presented here emphasises the presence of field bilinears $\Phi_a^\dagger \Phi_b$ in the scalar potential. It can be written as [19]

$$V_H = \sum_{\mu=0}^3 M_\mu r_\mu + \sum_{\mu,\nu=0}^3 \Lambda_{\mu\nu} r_\mu r_\nu, \quad (2.68)$$

where

$$\Lambda_{\mu\nu} = \Lambda_{\nu\mu} \quad (2.69)$$

and

$$\begin{aligned} r_0 &= \frac{1}{2}(\Phi_1^\dagger\Phi_1 + \Phi_2^\dagger\Phi_2) , \\ r_1 &= \frac{1}{2}(\Phi_1^\dagger\Phi_2 + \Phi_2^\dagger\Phi_1) = \Re(\Phi_1^\dagger\Phi_2) \\ r_2 &= -\frac{i}{2}(\Phi_1^\dagger\Phi_2 - \Phi_2^\dagger\Phi_1) = \Im(\Phi_1^\dagger\Phi_2) \\ r_3 &= \frac{1}{2}(\Phi_1^\dagger\Phi_1 - \Phi_2^\dagger\Phi_2) . \end{aligned} \quad (2.70)$$

This notation is convenient for studies of features such as the existence and number of minima of the scalar potential. Since the Yukawa couplings involve the Higgs doublets individually rather than bilinears, notation 3 cannot be applied for studies of the full theory with both scalars and fermions. The correspondence between notations 1 and 3 is given by

$$M_\mu = (m_{11}^2 + m_{22}^2, -2\Re(m_{12}^2), 2\Im(m_{12}^2), m_{11}^2 - m_{22}^2) , \quad (2.71)$$

$$\Lambda_{\mu\nu} = \begin{pmatrix} (\lambda_1 + \lambda_2)/2 + \lambda_3 & \Re(\lambda_6 + \lambda_7) & -\Im(\lambda_6 + \lambda_7) & (\lambda_1 - \lambda_2)/2 \\ \Re(\lambda_6 + \lambda_7) & \lambda_4 + \Re(\lambda_5) & -\Im(\lambda_5) & \Re(\lambda_6 - \lambda_7) \\ -\Im(\lambda_6 + \lambda_7) & -\Im(\lambda_5) & \lambda_4 - \Re(\lambda_5) & -\Im(\lambda_6 - \lambda_7) \\ (\lambda_1 - \lambda_2)/2 & \Re(\lambda_6 - \lambda_7) & -\Im(\lambda_6 - \lambda_7) & (\lambda_1 + \lambda_2)/2 - \lambda_3 \end{pmatrix} . \quad (2.72)$$

In the following we will discuss constraints on the 2HDM Higgs potential and the implications on its parameter values.

2.6.2 Stability of the 2HDM Potential

In order to ensure the stability of the 2HDM potential, we have to make sure that it is bounded from below, *i.e.* that there is no direction in field space along which the potential tends to minus infinity. The existence of a stable minimum, around which perturbative calculations can be performed, is a basic requirement for any physical theory. The scalar potential of the SM satisfies this requirement through the trivial condition $\lambda > 0$, where λ is the quartic coupling of the SM scalar potential. The 2HDM scalar potential of Eq. (2.64) is much more complicated than the one of the SM. All possible directions along which the fields Φ_1 and Φ_2 , respectively their eight component fields, tend to arbitrarily large values, have to be studied. In order to have a non-trivial minimum, *i.e.* the fields Φ_i acquire non-zero VEVs, two conditions have to be fulfilled: The quartic part of the scalar potential, V_4 , is positive for arbitrarily large values of the component fields, but the quadratic part of the scalar potential, V_2 , can take negative values for at least some values of the fields. In this respect, demanding $V_4 > 0$ for all $\Phi_i \rightarrow \infty$ may be a too strong requirement, since several interesting models are excluded by it. Thus in tree-level SUSY potentials there is a direction, $\langle \Phi_1 \rangle = \langle \Phi_2 \rangle$ for which $V_4 = 0$. A simple way to obtain *necessary* conditions on the quartic parameters of the potential is to study its behaviour along specific field directions. Considering for example the direction $|\Phi_1| \rightarrow \infty$ and $|\Phi_2| = 0$, the expression Eq. (2.64) for the potential obviously leads to the conclusion that one can have positive values for V_4 if and

only if $\lambda_1 \geq 0$. Likewise, the direction $|\Phi_1| = 0$ and $|\Phi_2| \rightarrow \infty$ gives the condition $\lambda_2 \geq 0$. By studying several such directions it is possible to reach other conditions on the couplings, arriving at

$$\begin{aligned} \lambda_1 &\geq 0, & \lambda_2 &\geq 0 \\ \lambda_3 &\geq -\sqrt{\lambda_1\lambda_2}, & \lambda_3 + \lambda_4 - |\lambda_5| &\geq -\sqrt{\lambda_1\lambda_2}, \end{aligned} \quad (2.73)$$

where λ_5 has been taken real. In potentials, where $\lambda_6 = \lambda_7 = 0$ these are actually necessary and sufficient conditions to ensure the positivity of the quartic potential along all directions.

The conditions Eq. (2.73) have been obtained through a tree-level analysis. The inclusion of higher order corrections is done by considering only the tree-level expressions Eq. (2.73), but taking the values of the couplings which appear in these expressions at different renormalization scales. One hence takes the bounds of Eq. (2.73) and runs the couplings therein, using the β -functions of the model along a range of scales μ , *i.e.* from the weak scale M_Z to an upper scale Λ . At all scales in the interval chosen the bounds must hold. Note, that combinations of parameters which at one scale might be acceptable would violate the bounds at another scale.

Such an analysis has been performed for the SM. The Higgs potential quartic coupling λ at the scale Q is given in terms of the β -function by

$$\frac{d\lambda}{d\ln Q} = \beta(g_i), \quad (2.74)$$

where g_i generically denotes the couplings of the model. The β -function is derived by considering the quantum corrections to the Higgs potential, and reads

$$\begin{aligned} 16\pi^2\beta &= 24\lambda^2 - (3g'^2 + 9g^2 - 12y_t^2)\lambda + \frac{3}{8}g'^4 + \frac{3}{4}g'^2g^2 + \frac{9}{8}g^4 - 6y_t^4 \\ &+ \text{higher order terms}. \end{aligned} \quad (2.75)$$

Here g and g' denote the SM electroweak gauge couplings and y_t the top Yukawa coupling. The β -function has a sizeable negative contribution from the top quark Yukawa coupling. As the top is so heavy, this term tends to decrease the value of λ at higher renormalization scales. If the starting value of λ at the weak scale is too small, the coupling can become negative at some higher scale and the potential would be unbounded from below. This allows us to put a lower bound on λ and thus on the Higgs mass. Let us have a closer look at this. For small masses (hence small $\lambda - g$ and g' are anyway small) the renormalization group equation (RGE) Eq. (2.75) is dominated by y_t , hence

$$16\pi^2\frac{d\lambda}{d\ln Q} = -6y_t^4. \quad (2.76)$$

Integration leads to

$$\lambda(Q) = \lambda_0 - \frac{\frac{3}{8\pi^2}y_0^4 \ln \frac{Q}{Q_0}}{1 - \frac{9}{16\pi^2}y_0^2 \ln \frac{Q}{Q_0}}. \quad (2.77)$$

Therefore λ decreases with Q . In order to have vacuum stability we have to require

$$\Lambda \leq v e^{4\pi^2 M_H^2 / (3y_t^4 v^2)}. \quad (2.78)$$

New Physics must appear before this point to ensure vacuum stability. For a fixed value of Λ this leads to a lower bound on M_H .

If the starting value of λ is too large, the RG evolution of the coupling will increase its value immensely and eventually the theory becomes non-perturbative. We will come back to this point later, when we discuss unitarity bounds. The RG analysis thus allows to impose higher and lower bounds on the masses of the Higgs particles.

In the 2HDM the same type of phenomena can occur. If for example the Φ_1 only couples to the up-type quarks, the β -function for the λ_1 quartic coupling will have a large negative top Yukawa contribution, and a similar analysis to the SM case will hold. However, in the 2HDM many other quartic couplings are present and more bounds need to be obeyed. Nevertheless the main conclusions hold: Smaller values for some of the λ_i at the weak scale are disfavoured as they lead to unbounded from below potentials at higher scales. Large values of these couplings lead to Landau poles at high scales and thus the breakdown of perturbation theory. These translate into bounds on the several Higgs masses.

2.6.3 Vacuum Stability

In the SM, apart from the trivial minimum, there is only *one* possible type of minimum. In the 2HDM, however, there exist three types of vacua:⁶

- “Normal” (N) vacua, with VEVs which do not have any complex relative phase and can thus trivially be rendered real:

$$\langle \Phi_1 \rangle_N = \begin{pmatrix} 0 \\ \frac{v_1}{\sqrt{2}} \end{pmatrix}, \quad \langle \Phi_2 \rangle_N = \begin{pmatrix} 0 \\ \frac{v_2}{\sqrt{2}} \end{pmatrix}, \quad (2.79)$$

where $v = \sqrt{v_1^2 + v_2^2} = 246$ GeV and $\tan \beta = v_2/v_1$.

- CP breaking vacua, where the VEVs have a relative complex phase,

$$\langle \Phi_1 \rangle_{CP} = \begin{pmatrix} 0 \\ \frac{\bar{v}_1}{\sqrt{2}} e^{i\theta} \end{pmatrix}, \quad \langle \Phi_2 \rangle_{CP} = \begin{pmatrix} 0 \\ \frac{\bar{v}_2}{\sqrt{2}} \end{pmatrix}, \quad (2.80)$$

where \bar{v}_1 and \bar{v}_2 are real.

- Charge breaking (CB) vacua, in which one of the VEVs carries electric charge,

$$\langle \Phi_1 \rangle_{CB} = \begin{pmatrix} \frac{\alpha}{\sqrt{2}} \\ \frac{v'_1}{\sqrt{2}} \end{pmatrix}, \quad \langle \Phi_2 \rangle_{CB} = \begin{pmatrix} 0 \\ \frac{v'_2}{\sqrt{2}} \end{pmatrix}, \quad (2.81)$$

with real numbers v'_1 , v'_2 , α . Because of the presence of a non-zero VEV in an upper component (charged) of the fields, this vacuum breaks electrical charge conservation, so that the photon acquires a mass. Such a vacuum therefore has to be avoided.

⁶Any stationary point of the potential, regardless of whether it is a minimum or not, is considered a vacuum.

The minima of the potential are defined by solving the minimization conditions. With the potential written in terms of \tilde{v}_i for any of the three sets Eqs. (2.79)-(2.81) a stationary point of the potential is found if the set of equations $\partial V/\partial\tilde{v}_i = 0$ has solutions. The different CP and CB stationary points are determined by a set of three equations and a normal one by only two. Since the 2HDM potential depends on eight real component fields, in fact, any stationary point should be the solution of a set of eight equations on eight unknowns. As one can always choose the simplified forms of the VEVs given in Eqs. (2.79)-(2.81), most of those equations are trivially satisfied. It has been shown in [20] that the charge breaking VEVs can always be obtained analytically and are given by

$$\begin{pmatrix} v_1'^2 + \alpha^2 \\ v_2'^2 \\ v_1'v_2' \end{pmatrix} = 2 \begin{pmatrix} \lambda_1 & \lambda_3 & 2\Re(\lambda_6) \\ \lambda_3 & \lambda_2 & 2\Re(\lambda_7) \\ 2\Re(\lambda_6) & 2\Re(\lambda_7) & 2(\lambda_4 + \Re(\lambda_5)) \end{pmatrix}^{-1} \begin{pmatrix} m_{11}^2 \\ m_{22}^2 \\ -2\Re(m_{12}^2) \end{pmatrix}. \quad (2.82)$$

This implies, that if Eq. (2.82) has a solution, then this is unique up to trivial sign changes ($\alpha \rightarrow -\alpha$, $v_1' \rightarrow -v_1'$, $v_2' \rightarrow -v_2'$) with no physical impact. Charge breaking is hence impossible in several symmetry-constrained 2HDM.

The CP breaking VEVs can be obtained analytically in terms of the parameters of the potential. Assuming potentials where the CP symmetry is defined one obtains

$$\begin{pmatrix} \bar{v}_1^2 \\ \bar{v}_2^2 \\ \bar{v}_1\bar{v}_2 \cos\theta \end{pmatrix} = 2 \begin{pmatrix} \lambda_1 & \lambda_3 + \lambda_4 - \Re(\lambda_5) & 2\Re(\lambda_6) \\ \lambda_3 + \lambda_4 - \Re(\lambda_5) & \lambda_2 & 2\Re(\lambda_7) \\ 2\Re(\lambda_6) & 2\Re(\lambda_7) & 4\Re(\lambda_5) \end{pmatrix}^{-1} \begin{pmatrix} m_{11}^2 \\ m_{22}^2 \\ -2\Re(m_{12}^2) \end{pmatrix} \quad (2.83)$$

Up to physically irrelevant sign changes the CP vacuum is unique.

The most difficult vacuum to be solved is the normal one. For many potentials the minimization conditions cannot be solved analytically. The equations $\partial V/\partial v_1 = 0$ and $\partial V/\partial v_2 = 0$ result for the most general 2HDM potential in

$$m_{11}^2 v_1 - \Re(m_{12}^2)v_2 + \frac{\lambda_1}{2}v_1^3 + \frac{\lambda_{345}}{2}v_1v_2^2 + \frac{1}{2}[3\Re(\lambda_6)v_1^2v_2 + \Re(\lambda_7)v_2^3] = 0 \quad (2.84)$$

$$m_{22}^2 v_2 - \Re(m_{12}^2)v_1 + \frac{\lambda_2}{2}v_2^3 + \frac{\lambda_{345}}{2}v_2v_1^2 + \frac{1}{2}[\Re(\lambda_6)v_1^3 + 3\Re(\lambda_7)v_2v_1^2] = 0, \quad (2.85)$$

with $\lambda_{345} = \lambda_3 + \lambda_4 + \Re(\lambda_5)$.

With the possibility of minima of different natures in theories with more than one scalar, the theory may allow for tunneling from one minimum to another. In the 2HDM therefore the question arises: Can the vacua of different natures coexist with one another? Could one tunnel from a normal minimum to a deeper charge-breaking one? In other words, given a minimum in the 2HDM, is it stable? In Refs. [20, 21, 22] it has been shown:

- Suppose we have a potential where a normal stationary point and a charge breaking one exist, and with the VEVs given by Eqs. (2.82) and (2.84), (2.85), then the difference in the values of the scalar potential at both those vacua is given by

$$V_{CB} - V_N = \left(\frac{M_{H^\pm}^2}{4v^2} \right)_N \underbrace{[(v_1'v_2 - v_2'v_1)^2 + \alpha^2v_2^2]}_{>0}. \quad (2.86)$$

Note that $(M_{H^\pm}^2/v^2)_N$ is the ratio of the squared mass of the charged scalar to the sum of the square of the VEVs, $v^2 = v_1^2 + v_2^2$, as computed in the normal stationary point. This implies: If the normal stationary point is a minimum, which implies $M_{H^\pm}^2 > 0$, then one will necessarily have $V_{CB} - V_N > 0$. Hence, if there is a normal minimum, any CB stationary point will lie above it. The normal minimum is stable against charge breaking. It was also proven in [20] that in such a case the CB stationary point is necessarily a saddle point. Therefore normal and CB minima cannot co-exist in the 2HDM. In case the set of parameters is chosen such that the global minimum of the potential breaks charge, there are no normal minima.

- In case we have a potential where a normal stationary point and a CP breaking one exist with the VEVs given by Eqs. (2.83) and (2.84), (2.85), the difference in the values of the scalar potential at both those vacua is given by

$$V_{CP} - V_N = \left(\frac{M_A^2}{4v^2} \right)_N \underbrace{[(\bar{v}_1 v_2 \cos \theta - \bar{v}_2 v_1)^2 + \bar{v}_1^2 v_2^2 \sin^2 \theta]}_{>0}. \quad (2.87)$$

Note that $(M_A^2/4v^2)_N$ is the ratio of the squared mass of the pseudoscalar to the sum of the square of the VEVs, $v^2 = v_1^2 + v_2^2$, as computed in the normal stationary point. Therefore, if the normal stationary point is a minimum, which implies that $M_A^2 > 0$ then we necessarily have $V_{CP} - V_N > 0$. If there is a normal minimum, any CP stationary point will hence be above it. The normal minimum is stable against CP breaking. In [23] it was proven that in that case the CP stationary point is necessarily a saddle point, and therefore normal and CP minima cannot co-exist in the 2HDM. If the set of parameters of the potential is chosen such that the global minimum of the potential breaks CP, then there are no normal minima.

- Also no CB and CP minima can co-exist. This is because for the CP vacuum the square of the charged Higgs mass is given by

$$(M_{H^\pm}^2)_{CP} = -\frac{1}{2}[\lambda_4 - \Re(\lambda_5)](\bar{v}_1^2 + \bar{v}_2^2), \quad (2.88)$$

whereas in a CB vacuum one of the squared mass matrix eigenvalues is

$$M_{CB}^2 = \frac{1}{2}[\lambda_4 - \Re(\lambda_5)](v_1'^2 + v_2'^2 + \alpha^2). \quad (2.89)$$

The sign of $\lambda_4 - \Re(\lambda_5)$ determines that both these vacua cannot be simultaneously minima. Therefore if a CP minimum exists the (unique) CB stationary point, if it exists, cannot be a minimum as well, and vice-versa.

- The normal minimization conditions, however, allow for multiple solutions, so that one can have an N_1 vacuum with VEVs $\{v_{1,1}, v_{2,1}\}$ and an N_2 vacuum with different VEVs $\{v_{1,2}, v_{2,2}\}$. The difference in the values of the potential in these two vacua is given by

$$V_{N_2} - V_{N_1} = \frac{1}{4} \left[\left(\frac{M_{H^\pm}^2}{v^2} \right)_{N_1} - \left(\frac{M_{H^\pm}^2}{v^2} \right)_{N_2} \right] (v_{1,1} v_{2,2} - v_{2,1} v_{1,2})^2, \quad (2.90)$$

where $(M_{H^\pm}^2/v^2)_{N_1}$ is the ratio of the charged mass squared to the sum of the square VEVs, $(v^2)_{N_1} = v_{1,1}^2 + v_{2,1}^2$, as computed in the N_1 stationary point, and analogously for $(M_{H^\pm}^2/v^2)_{N_2}$. This equation shows that nothing favours N_1 over N_2 . The deepest stationary point is simply determined by the values of the parameters. This is to be expected as the two vacua have the same symmetries. It was proven in [23] that it is possible to have two co-existing normal minima. On the other hand it is very easy to find a set of parameters where N_1 would be the global minimum, with N_2 above it or not even existing.

In summary, for the 2HDM vacua the following holds:

- Minima of different natures cannot coexist in the 2HDM.
- Whenever a normal minimum exists in the 2HDM, the global minimum of the potential is normal. No tunneling to a deeper CB or CP minimum is possible.
- If a CP (CB) violating minimum exists, it is the global minimum of the theory and thoroughly stable. No tunnelling to a deeper normal or CB (CP) minimum can occur.

2.6.4 Unitarity Constraints

We have already seen that the condition that the potential must have a minimum and is not unbounded from below leads to constraints on the parameter values of the Higgs potential. Another theoretical constraint arises from the requirement, that all the (tree-level) scalar-scalar scattering amplitudes must respect unitarity. In the SM this requirement is equivalent to ensuring that the quartic coupling in the scalar potential is not too large. This leads then to an upper bound on the Higgs boson mass. We can see this by looking again at the RGE in Eq. (2.75). For large masses (and hence large λ), the RGE is dominated by the λ term, hence

$$16\pi^2 \frac{d\lambda}{d \ln Q} = 24\lambda^2. \quad (2.91)$$

This is solved by

$$\lambda(Q) = \frac{M_H^2}{2v^2 - \frac{3}{2\pi^2} M_H^2 \ln \frac{Q}{v}}. \quad (2.92)$$

The coupling λ hence increases with Q . It diverges at the Landau pole. We therefore have to require that new physics appears before this point, in order to restore stability, hence

$$\Lambda \leq v e^{4\pi^2 v^2 / (3M_H^2)}. \quad (2.93)$$

For fixed Λ this translates into an upper bound on M_H . Extending this bound to the 2HDM is complicated. Due to the richer scalar spectrum many scattering amplitudes need to be taken into account. Furthermore the existence of many quartic couplings makes things more complicated. This leads to an analysis of the eigenvalues of the S matrix for scalar-scalar

scattering amplitudes. The relevant ones are given by

$$a_{\pm} = \frac{3}{2}(\lambda_1 + \lambda_2) \pm \sqrt{\frac{9}{4}(\lambda_1 - \lambda_2)^2 + (2\lambda_3 + \lambda_4)^2}, \quad (2.94)$$

$$b_{\pm} = \frac{1}{2}(\lambda_1 + \lambda_2) \pm \frac{1}{2}\sqrt{(\lambda_1 - \lambda_2)^2 + 4\lambda_4^2}, \quad (2.95)$$

$$c_{\pm} = \frac{1}{2}(\lambda_1 + \lambda_2) \pm \frac{1}{2}\sqrt{(\lambda_1 - \lambda_2)^2 + 4\lambda_5^2}, \quad (2.96)$$

$$e_1 = \lambda_3 + 2\lambda_4 - 3\lambda_5, \quad (2.97)$$

$$e_2 = \lambda_3 - \lambda_5, \quad (2.98)$$

$$f_+ = \lambda_3 + 2\lambda_4 + 3\lambda_5, \quad (2.99)$$

$$f_- = \lambda_3 + \lambda_5, \quad (2.100)$$

$$f_1 = \lambda_3 + \lambda_4, \quad (2.101)$$

$$p_1 = \lambda_3 - \lambda_4. \quad (2.102)$$

The requirement of tree-level perturbative unitarity leads to

$$|a_{\pm}|, |b_{\pm}|, |c_{\pm}|, |f_{\pm}|, |e_{1,2}|, |f_1|, |p_1| < 8\pi. \quad (2.103)$$

2.6.5 Further Constraints

The Higgs bosons of the 2HDM also contribute to the electroweak precision observables. New physics contributions to these observables can conveniently be parametrized in terms of the oblique parameters. With the vacuum polarization tensors written as

$$\Pi_{VV'}^{\mu\nu}(q) = g^{\mu\nu} A_{VV'}(q^2) + q^{\mu} q^{\nu} B_{VV'}(q^2), \quad (2.104)$$

where VV' is either $\gamma\gamma$, γZ , ZZ or W^+W^- and $q = (q^{\alpha})$ is the four-momentum of the gauge bosons, and defining

$$\bar{A}_{VV'}(q^2) = A_{VV'}(q^2)|_{2\text{HDM}} - A_{VV'}(q^2)|_{\text{SM}}, \quad (2.105)$$

the oblique parameters S, T, U, V, W, X of the 2HDM can be expressed in terms of the $\bar{A}_{VV'}$. Electroweak precision constraints lead to

$$m_A = m_{H^{\pm}} \quad (2.106)$$

$$\sin(\beta - \alpha) = 1 \quad \Rightarrow \quad m_{H^{\pm}} = m_H \quad (2.107)$$

$$\sin(\beta - \alpha) = 0 \quad \Rightarrow \quad m_{H^{\pm}} = m_h. \quad (2.108)$$

Other constraints arise from the measurement of muon anomalous magnetic moment and from B -physics. In particular the charged Higgs boson can have a significant effect on B -physics observables. For all four models without FCNC the Yukawa couplings of the charged Higgs boson can be written as

$$\mathcal{L}_{H^{\pm}} = -H^+ \left(\frac{\sqrt{2}V_{ud}}{v} \bar{u}(m_u X P_L + m_d Y P_R)d + \frac{\sqrt{2}m_l}{\nu} Z \bar{\nu}_L l_R \right) + \text{h.c.} . \quad (2.109)$$

The values of X, Y and Z are given in Table 2.2 for the various models. In Type I the couplings to all fermions are suppressed if $\tan\beta \gg 1$, implying a fermiophobic charged

	Type I	Type II	Lepton-specific	Flipped
X	$\cot \beta$	$\cot \beta$	$\cot \beta$	$\cot \beta$
Y	$\cot \beta$	$-\tan \beta$	$\cot \beta$	$-\tan \beta$
Z	$\cot \beta$	$-\tan \beta$	$-\tan \beta$	$\cot \beta$

Table 2.2: The parameters X , Y and Z for the four models without FCNC.

Higgs. In the same limit one has in the lepton-specific model a quark-phobic but lepto-philic charged Higgs, which could lead to a huge branching ratio for $H^\pm \rightarrow \tau^\pm \nu_\tau$. In both models the quark-phobic nature of the charged Higgs eliminates constraints from rare B decays. In the type II and flipped model large contributions to rare B decays are possible. The data on $B \rightarrow X_s \gamma$ lead for these models then to a constraint on the charged Higgs mass given by [24]

$$m_{H^\pm} \gtrsim 580 \text{ GeV} . \quad (2.110)$$

All models are constraint by the data on $B_d^0 - \bar{B}_d^0$ and $B_s^0 - \bar{B}_s^0$ mixing. The measured

$$R_b = \frac{\Gamma(Z \rightarrow b\bar{b})}{\Gamma(Z \rightarrow q\bar{q})} \quad (2.111)$$

constrains

$$\tan \beta \gtrsim 1 . \quad (2.112)$$

Last but not least there are constraints from the Higgs data from LEP, Tevatron and LHC. It has to be made sure that the 2HDM Higgs sector is not in conflict with the reported exclusion limits and the Higgs data of the discovered 126 GeV scalar. Thus at LEP it was looked for the production of charged Higgs bosons in

$$e^+ e^- \rightarrow H^+ H^- , \quad (2.113)$$

with the charged Higgs decaying into $\tau^\pm \nu_\tau$. For any model the non-observation of the charged Higgs leads then to a constraint of $m_{H^\pm} \gtrsim 80 \text{ GeV}$. And for the lepton-specific one, the limit is $m_{H^\pm} \gtrsim 94 \text{ GeV}$. At ATLAS and CMS a charged Higgs boson is looked for in

$$pp \rightarrow t\bar{t} \rightarrow \bar{b}b W^+ H^- . \quad (2.114)$$

The non-observation translates into exclusion limits in the $\tan \beta - m_{H^\pm}$ plane.

There are dedicated public programs available that allow to check for the Higgs data constraints, namely `HiggsBounds` [25, 26, 27] and `HiggsSignals` [28]. The program `HiggsBounds` requires as inputs the effective couplings of the Higgs bosons of the investigated model, normalized to the corresponding SM values, as well as the masses, the widths and the branching ratios of the Higgs bosons. This allows then to check for the compatibility with the non-observation of the 2HDM Higgs bosons, in particular whether or not the Higgs spectrum is excluded at the 95% confidence level (CL) in view of the LEP, Tevatron and LHC measurements. The package `HiggsSignals` uses the same input and validates the compatibility of the SM-like Higgs boson with the Higgs observation data. A p -value is given, which when demanded to be at least 0.05 corresponds to a non-exclusion at 95% CL.

A tool for performing scans of the parameter space of scalar sectors is given by `ScannerS` [32]. It automatises scans for tree-level renormalizable scalar potentials. It is interfaced with

- **SuShi** [29] for the Higgs production at NNLO in gluon fusion and associated production with bb .
- **HDECAY** [30] for the computation of the Higgs decays.
- **Superiso** [31] for the check of some flavour physics observables.
- **HiggsBounds** for the limits from the Higgs searches at LEP, Tevatron and the LHC.
- **HiggsSignals** for the signal rates at the Tevatron and LHC.

Furthermore **ScannerS** checks for the global minimum and has implemented checks of the constraints from vacuum stability (potential bounded from below), unitarity, electroweak precision observables and some alternative sources for B -physics constraints. The webpage of the program is given by:

<http://www.hepforge.org/archive/scanners/>

In order to check for the 2HDM allowed parameter space with the available LHC data as given in September 2014, a random scan has been performed, setting $m_h = 125.9$ GeV, over the parameter values

$$\begin{aligned}
50 \text{ GeV} &\leq m_{H^\pm} \leq 1 \text{ TeV} \\
m_h + 5 \text{ GeV} &\leq m_A, m_H \leq 1 \text{ TeV} \\
-900^2 \text{ GeV}^2 &\leq m_{12}^2 \leq 900^2 \text{ GeV}^2 \\
0.5 &\leq \tan \beta \leq 50 \\
-\frac{\pi}{2} &\leq \alpha \leq \frac{\pi}{2}.
\end{aligned} \tag{2.115}$$

The theoretical and pre-LHC experimental constraints have been imposed. The branching ratios and production rates at the LHC have been calculated and the collider constraints have been checked with **HiggsBounds** and **HiggsSignals**. The result for the type II model is shown in Fig. 2.1. As can be inferred from the plot there are two regions that are favoured. One is given by the SM-like limit. Here $\sin(\beta - \alpha) = 1$, leading to $\kappa_F = 1$ and $\kappa_V = 1$, where κ_x denotes the 2HDM coupling of the SM-like h with mass around 125 GeV to the SM particles x normalized to the corresponding coupling of the SM Higgs boson with same mass. Hence all tree-level coupling to fermions and massive gauge bosons are as in the SM. The other favoured region is the so-called 'wrong-sign' limit [33], as here

$$\kappa_D \kappa_V < 0 \quad \text{or} \quad \kappa_U \kappa_V < 0. \tag{2.116}$$

This means that the Yukawa couplings and couplings to massive gauge bosons have a relative minus sign. This can be easily checked by re-writing the coupling factor κ_D to down-type fermions, which in the type II model is given by

$$\kappa_D = -\frac{\sin \alpha}{\cos \beta} = -\sin(\beta + \alpha) + \cos(\beta + \alpha) \tan \beta \tag{2.117}$$

and analogously

$$\kappa_U = \frac{\cos \alpha}{\sin \beta} = \sin(\beta + \alpha) + \cos(\beta + \alpha) \cot \beta. \tag{2.118}$$

For $\sin(\beta + \alpha) = 1$ this leads to $\kappa_D = -1$ ($\kappa_U = 1$) and with

$$\kappa_V = \sin(\beta - \alpha) = \frac{\tan^2 \beta - 1}{\tan^2 \beta + 1} \tag{2.119}$$

we have $\kappa_V \geq 0$ if $\tan \beta \geq 1$.

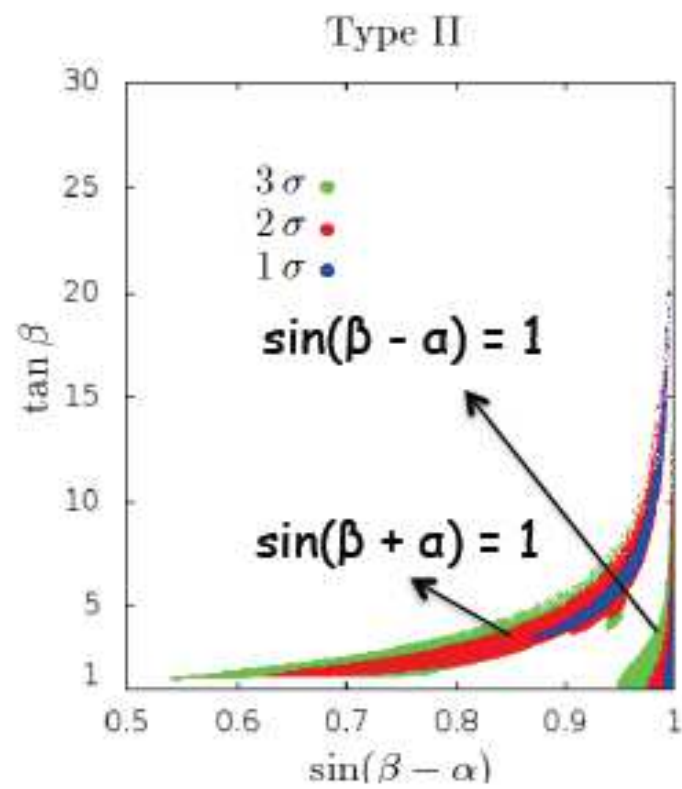


Figure 2.1: Allowed parameters space of the type II 2HDM model as in September 2014. Taken from the talk given by R. Santos at HiggsDays 2014 in Santander.

Chapter 3

Appendix

3.1 Beispiel: Feldtheorie für ein komplexes Feld

Wir betrachten die Lagrangedichte für ein komplexes Skalarfeld

$$\mathcal{L} = (\partial_\mu \phi)^* (\partial^\mu \phi) - \mu^2 \phi^* \phi - \lambda (\phi^* \phi)^2 \quad \text{mit dem Potential} \quad V = \mu^2 \phi^* \phi + \lambda (\phi^* \phi)^2. \quad (3.1)$$

(Hinzufügen höherer Potenzen in ϕ führt zu einer nicht-renormierbaren Theorie.) Die Lagrangedichte ist invariant unter einer $U(1)$ -Symmetrie,

$$\phi \rightarrow \exp(i\alpha) \phi. \quad (3.2)$$

Wir betrachten den Grundzustand. Dieser ist gegeben durch das Minimum von V ,

$$0 = \frac{\partial V}{\partial \phi^*} = \mu^2 \phi + 2\lambda (\phi^* \phi) \phi \quad \Rightarrow \quad \phi = \begin{cases} 0 & \text{für } \mu^2 > 0 \\ \phi^* \phi = -\frac{\mu^2}{2\lambda} & \text{für } \mu^2 < 0 \end{cases} \quad (3.3)$$

Der Parameter λ muß positiv sein, damit das System nicht instabil wird. Für $\mu^2 < 0$ nimmt das Potential die Form eines Mexikanerhutes an, siehe Fig. 3.1. Bei $\phi = 0$ liegt ein lokales Maximum, bei

$$|\phi| = v = \sqrt{-\frac{\mu^2}{2\lambda}} \quad (3.4)$$

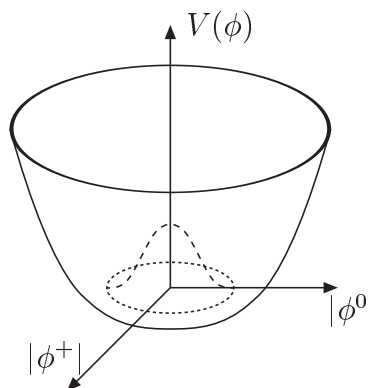


Figure 3.1: Das Higgspotential.

ein globales Minimum. Teilchen entsprechen harmonischen Oszillatoren für die Entwicklung um das Minimum des Potentials. Fluktuationen in Richtung der (unendlich vielen degenerierten) Minima besitzen Steigung null und entsprechen masselosen Teilchen, den Goldstone Bosonen. Fluktuationen senkrecht zu dieser Richtung entsprechen Teilchen mit Masse $m > 0$. Die Entwicklung um das Maximum bei $\phi = 0$ würde zu Teilchen negativer Masse (Tachyonen) führen, da die Krümmung des Potentials hier negativ ist.

Entwicklung um das Minimum bei $\phi = v$ führt zu (wir haben für das komplexe skalare Feld zwei Fluktuationen φ_1 und φ_2)

$$\phi = v + \frac{1}{\sqrt{2}}(\varphi_1 + i\varphi_2) = \left(v + \frac{1}{\sqrt{2}}\varphi_1\right) + i\frac{\varphi_2}{\sqrt{2}} \quad \Rightarrow \quad (3.5)$$

$$\phi^*\phi = v^2 + \sqrt{2}v\varphi_1 + \frac{1}{2}(\varphi_1^2 + \varphi_2^2). \quad (3.6)$$

Damit erhalten wir für das Potential

$$V = \lambda(\phi^*\phi - v^2)^2 - \frac{\mu^4}{4\lambda^2} \quad \text{mit} \quad v^2 = -\frac{\mu^2}{2\lambda} \quad \Rightarrow \quad (3.7)$$

$$V = \lambda \left(\sqrt{2}v\varphi_1 + \frac{1}{2}(\varphi_1^2 + \varphi_2^2) \right)^2 - \frac{\mu^4}{4\lambda^2}. \quad (3.8)$$

Vernachlässige den letzten Term in V , da es sich nur um eine konstante Nullpunktsverschiebung handelt. Damit ergibt sich für die Lagrangedichte

$$\mathcal{L} = \frac{1}{2}(\partial_\mu\varphi_1)^2 + \frac{1}{2}(\partial_\mu\varphi_2)^2 - 2\lambda v^2\varphi_1^2 - \sqrt{2}v\lambda\varphi_1(\varphi_1^2 + \varphi_2^2) - \frac{\lambda}{4}(\varphi_1^2 + \varphi_2^2)^2. \quad (3.9)$$

Die in den Feldern quadratischen Terme liefern die Massen, die in den Feldern kubischen und quartischen Terme sind die Wechselwirkungsterme. Es gibt ein massives und ein masseloses Teilchen,

$$m_{\varphi_1} = 2v\sqrt{\lambda} \quad \text{und} \quad m_{\varphi_2} = 0. \quad (3.10)$$

Bei dem masselosen Teilchen handelt es sich um das Goldstone Boson.

Bibliography

- [1] J. Goldstone, A. Salam and S. Weinberg, Phys. Rev. **127** (1962) 965; S. Weinberg, Phys. Rev. Lett. **19** (1967) 1264; S.L. Glashow, S. Weinberg, Phys. Rev. Lett. **20** (1968) 224; A. Salam, Proceedings Of The Nobel Symposium, Stockholm 1968, ed. N. Svartholm.
- [2] P.W. Higgs, Phys. Lett. **12** (1964) 132; Phys. Rev. Lett. **13** (1964) 508 and Phys. Rev. **145** (1966) 1156; F. Englert and R. Brout, Phys. Rev. Lett. **13** (1964) 321; G.S. Guralnik, C.R. Hagen and T.W. Kibble, Phys. Rev. Lett. **13** (1964) 585.
- [3] G. Aad *et al.* [ATLAS Collaboration], Phys. Lett. B **716** (2012) 1 doi:10.1016/j.physletb.2012.08.020 [arXiv:1207.7214 [hep-ex]].
- [4] S. Chatrchyan *et al.* [CMS Collaboration], Phys. Lett. B **716** (2012) 30 doi:10.1016/j.physletb.2012.08.021 [arXiv:1207.7235 [hep-ex]].
- [5] A. Djouadi, J. Kalinowski and M. Spira, Comput. Phys. Commun. **108** (1998) 56 doi:10.1016/S0010-4655(97)00123-9 [hep-ph/9704448].
- [6] A. Djouadi, J. Kalinowski, M. Muehlleitner and M. Spira, arXiv:1801.09506 [hep-ph].
- [7] S. Dittmaier *et al.*, doi:10.5170/CERN-2012-002 arXiv:1201.3084 [hep-ph].
- [8] S. Heinemeyer *et al.* [LHC Higgs Cross Section Working Group], doi:10.5170/CERN-2013-004 arXiv:1307.1347 [hep-ph].
- [9] D. de Florian *et al.* [LHC Higgs Cross Section Working Group], doi:10.23731/CYRM-2017-002 arXiv:1610.07922 [hep-ph].
- [10] S. Kanemura, Y. Okada, E. Senaha and C.-P. Yuan, Phys. Rev. D **70** (2004) 115002 [hep-ph/0408364].
- [11] G. C. Branco, P. M. Ferreira, L. Lavoura, M. N. Rebelo, M. Sher and J. P. Silva, Phys. Rept. **516** (2012) 1 [arXiv:1106.0034 [hep-ph]].
- [12] J.F. Gunion, H. Haber, G. Kane and S. Dawson, “*The Higgs Hunter’s Guide*”, Perseus Books, 1990.
- [13] S. L. Glashow and S. Weinberg, Phys. Rev. D **15** (1977) 1958.
- [14] S. L. Glashow and S. Weinberg, Phys. Rev. D **15** (1977) 1958; E. A. Paschos, Phys. Rev. D **15** (1977) 1966.
- [15] M. Aoki, S. Kanemura, K. Tsumura and K. Yagyu, Phys. Rev. D **80** (2009) 015017 [arXiv:0902.4665 [hep-ph]].

-
- [16] S. Davidson and H.E. Haber, Phys. Rev. **D72**, 035004 (2005); Erratum-ibid. **D72**, 099902 (2005); I.F. Ginzburg and M. Krawczyk, Phys. Rev. **D72**, 115013 (2005). F.J. Botella and J.P. Silva, Phys. Rev. **D51**, 3870 (1995).
- [17] Y. L. Wu and L. Wolfenstein, Phys. Rev. Lett. **73** (1994) 1762 [hep-ph/9409421].
- [18] F. J. Botella and J. P. Silva, Phys. Rev. D **51** (1995) 3870 [hep-ph/9411288].
- [19] C. C. Nishi, Phys. Rev. D **74** (2006) 036003 [Erratum-ibid. D **76** (2007) 119901] [hep-ph/0605153].
- [20] P. M. Ferreira, R. Santos and A. Barroso, Phys. Lett. B **603** (2004) 219 [Erratum-ibid. B **629** (2005) 114] [hep-ph/0406231].
- [21] A. Barroso, P. M. Ferreira and R. Santos, Phys. Lett. B **632** (2006) 684 [hep-ph/0507224].
- [22] A. Barroso, P. M. Ferreira, R. Santos and J. P. Silva, Phys. Rev. D **74** (2006) 085016 [hep-ph/0608282].
- [23] I. P. Ivanov, Phys. Rev. D **77** (2008) 015017 [arXiv:0710.3490 [hep-ph]].
- [24] M. Misiak and M. Steinhauser, Eur. Phys. J. C **77** (2017) no.3, 201 doi:10.1140/epjc/s10052-017-4776-y [arXiv:1702.04571 [hep-ph]].
- [25] P. Bechtle, O. Brein, S. Heinemeyer, G. Weiglein and K. E. Williams, Comput. Phys. Commun. **181** (2010) 138 [arXiv:0811.4169 [hep-ph]].
- [26] P. Bechtle, O. Brein, S. Heinemeyer, G. Weiglein and K. E. Williams, Comput. Phys. Commun. **182** (2011) 182 [arXiv:1102.1898 [hep-ph]].
- [27] P. Bechtle, O. Brein, S. Heinemeyer, O. Stål, T. Stefaniak et al., Eur. Phys. J C **74** (2014) 2693 [arXiv:1311.0055 [hep-ph]].
- [28] P. Bechtle, S. Heinemeyer, O. Stål, T. Stefaniak and G. Weiglein, Eur. Phys. J C **74** (2014) 2711 [arXiv:1305.1933 [hep-ph]].
- [29] R. V. Harlander, S. Liebler and H. Mantler, Comp. Phys. Commun. **184** (2013) 1605 [arXiv:1212.3249 [hep-ph]].
- [30] A. Djouadi, M. Spira and P.M. Zerwas, Phys. Lett. B **264** (1991) 440 and Z. Phys. C **70** (1996) 427; M. Spira *et al.*, Nucl. Phys. B **453** (1995) 17; A. Djouadi, J. Kalinowski and M. Spira, Comput. Phys. Commun. **108** (1998) 56; J. M. Butterworth, A. Arbey, L. Basso, S. Belov, A. Bharucha, F. Braam, A. Buckley and M. Campanelli *et al.*, arXiv:1003.1643 [hep-ph].
- [31] F. Mahmoudi, Comput. Phys. Commun. **178** (2008) 745 [arXiv:0710.2067 [hep-ph]]; F. Mahmoudi, Comput. Phys. Commun. **180** (2009) 1579 [arXiv:0808.3144 [hep-ph]].
- [32] R. Coimbra, M. O. P. Sampaio and R. Santos, Eur. Phys. J. C **73** (2013) 2428 [arXiv:1301.2599].

-
- [33] P. M. Ferreira, J. F. Gunion, H. E. Haber and R. Santos, *Phys. Rev. D* **89** (2014) 115003 [arXiv:1403.4736 [hep-ph]]; P. M. Ferreira, R. Guedes, M. O. P. Sampaio and R. Santos, arXiv:1409.6723 [hep-ph].
- [34] M. Muhlleitner, M. O. P. Sampaio, R. Santos and J. Wittbrodt, *JHEP* **1708** (2017) 132 doi:10.1007/JHEP08(2017)132 [arXiv:1703.07750 [hep-ph]].
- [35] R. Contino, Y. Nomura and A. Pomarol, *Nucl. Phys. B* **671** (2003) 148 [hep-ph/0306259].
- [36] K. Agashe, R. Contino and A. Pomarol, *Nucl. Phys. B* **719** (2005) 165 [hep-ph/0412089].
- [37] R. Contino, L. Da Rold and A. Pomarol, *Phys. Rev. D* **75** (2007) 055014 [hep-ph/0612048].